Endocranial anatomy and life habits of the Early Triassic archosauriform Proterosuchus fergusi

Brown, Emily; Butler, Richard; Ezcurra, Martin; Bhullar, Bhart-Anjan; Lautenschlager, Stephan

DOI:
10.1111/pala.12454

Endocranial anatomy and life habits of the Early Triassic archosauriform *Proterosuchus fergusi*

EMILY E. BROWN[1*], RICHARD J. BUTLER[1], MARTÍN D. EZCURRA[1,2], BHART-ANJAN S. BHULLAR[3], STEPHAN LAUTENSCHLAGER[1*]

[1]School of Geography, Earth and Environmental Sciences, University of Birmingham, Birmingham, United Kingdom

[2]Sección Paleontología de Vertebrados, CONICET−Museo Argentino de Ciencias Naturales "Bernardino Rivadavia", Buenos Aires, Argentina

[3]Department of Geology and Geophysics, Yale University, New Haven, Connecticut, USA

*Corresponding authors: emilyb62@hotmail.com, s.lautenschlager@bham.ac.uk

Abstract: Proterosuchids are an important group of carnivorous basal archosauriforms characterised by a bizarre and enigmatic downturned premaxilla that overhangs the lower jaw. They are particularly significant because they radiated in the immediate aftermath of the Permian–Triassic mass extinction, and represent one of the best known 'disaster taxa' following that event. While traditionally considered semi-aquatic, recent histological studies and geological data have suggested that they more likely inhabited terrestrial environments. By utilising computed tomographic (CT) data, we virtually reconstruct the brain endocast and endosseous labyrinths of two adult specimens of *Proterosuchus fergusi* from the earliest Triassic of South Africa, in an attempt to understand its life habits within the context of basal

archosauriform evolution. Endocasts reveal that the brain cavity is tubular in shape and the endosseous labyrinths are highly pyramidal. The angle of the lateral semi-circular canal suggests that *P. fergusi* naturally held its head upwards ~17°, while the length of the cochlear duct suggests its auditory abilities were specialised towards low-frequency sounds. Furthermore, beam theory analysis suggests that the rostrum of *P. fergusi* is highly resistant to both bending and torsion when compared to modern crocodilians, although this resistance is neither enhanced or reduced by the overhanging premaxilla. Comparative anatomical analyses suggest *P. fergusi* was likely a semi-aquatic, generalist apex predator capable of surviving the harsh environmental perturbations of the Early Triassic.

KEYWORDS: Archosauriformes, endocranial anatomy, brain cavity, semi-circular canals, digital reconstruction, Early Triassic

The end-Permian mass extinction is thought to have resulted in the loss of up to ~96% of life on Earth, including ~70% of terrestrial vertebrates (Raup 1979; Jablonski 1995; Benton & Twitchett 2003; Chen & Benton 2012). Despite the desolate greenhouse conditions of the Early Triassic, the opening up of new ecosystems and niches allowed for an adaptive radiation of surviving clades (Chen & Benton 2012; Viglietti *et al.* 2013; Foth *et al*. 2016; Ezcurra & Butler 2018). Originating in the middle–late Permian, the diapsid clade Archosauriformes successfully gained a foothold in the Early Triassic world, and gave rise to groups that would go on to dominate in the Mesozoic (e.g. crocodylomorphs, dinosaurs, pterosaurs) as well as continuing to make up a considerable portion of the modern fauna (e.g. birds, crocodylians) (Ezcurra *et al*. 2014; Pinheiro *et al.* 2016; Ezcurra & Butler 2018).

The basal archosauriform group Proterosuchidae, characterised by an enigmatic downturned premaxilla that overhangs the anterior margin of the lower jaw, is often referred to as a 'disaster' clade that thrived for a geologically short interval following the end-Permian extinction (e.g. Ezcurra 2016; Button *et al*. 2017). The clade attained a near cosmopolitan distribution, with specimens found in China, India, and South Africa (Ezcurra *et al.* 2013; Ezcurra 2016). The type species of this clade, *Proterosuchus fergusi* Broom 1903, is known from the *Lystrosaurus* Assemblage Zone (AZ) of the Karoo Supergroup of South Africa. Although well sampled, with eleven highly informative specimens, many aspects of the species' life habits and functional morphology are still unknown (Ezcurra & Butler 2015a). Traditionally, *P. fergusi* was considered semi-aquatic due to its superficial similarity to modern crocodylians and the then-presumed wet climate of the Early Triassic Karoo Basin (Broili & Schröder 1934; Tatarinov 1961; Reig 1970). Further evidence for an aquatic affinity included the predominately horizontal orientation of vertebral zygapophyses, allowing for lateral flexure of the body, which crocodiles use to propel themselves through the water (Cruickshank 1972).

However, proterosuchid ecology has since been disputed, with several authors suggesting a more terrestrial life habit (Cruickshank 1972; Welman 1998; Botha-Brink & Smith 2011). Cruickshank (1972) and Welman (1998) noted the lack of dorsally positioned external nares, which are an adaptation typical of aquatic and semi-aquatic diapsids such as plesiosaurs, mosasaurs, phytosaurs and crocodylians (Sereno 1991; Nesbitt *et al.* 2009). Cruickshank (1972) also noted the presence of well-ossified limbs, carpus and tarsus, and the vertical orientation of the occipital elements, and suggested *P. fergusi* was largely terrestrial. Furthermore, Botha-Brink & Smith (2011) combined sedimentological data and an osteohistological analysis of several *P. fergusi* limb bones, which provided no evidence of osteological specialisation to aquatic life (such as pachyosteosclerosis or osteoporosis), to

suggest a terrestrial mode of life for this species. However, palaeohistological analyses are not always accurately indicative of ecology, with, for example, a similar study finding no aquatic osteological specialisations in the marine teleosaurids, *Steneosaurus* and *Teleosaurus* (Hua & De Buffrenil 1996).

Proterosuchus fergusi is both the earliest new tetrapod following the onset of the Triassic and the best-sampled basal archosauriform species from the Karoo Basin (Smith & Botha 2005; Botha-Brink & Smith 2011; Smith *et al.* 2012). Therefore, consensus on the life habits of this species is crucial to understanding the faunal recovery following the end-Permian mass extinction. While the neuroanatomy and inner ear morphology of archosaurs have been extensively studied, non-archosaurian archosauromorphs have been widely neglected, in part due to their comparatively poor fossil record. To date, the brain endocast of only one basal archosauriform has been described in the literature, the proterochampsian *Tropidosuchus romeri* (Trotteyn & Paulina-Carabajal 2016). Several basal archosauriform endosseous labyrinths have been virtually reconstructed (Sobral *et al*. 2016a; Trotteyn & Paulina-Carabajal 2016); however, none are complete.

This study presents the first in-depth assessment of the endocranial anatomy of the basal archosauriform *P. fergusi*. Based on data from the endocranial reconstructions, we further discuss the life habits and ecology of *P. fergusi* and implications for the early evolution of Archosauriformes.

METHODS

Specimens

The skulls of two specimens of *Proterosuchus fergusi* were used in this study, RC 846 (Rubidge Collection, Wellwood, Graaff-Reinet, South Africa) and SNSB-BSPG 1934 VIII

514 (Staatliche Naturwissenschaftliche Sammlungen Bayerns/Bayerische Staatssammlung für Paläontologie und Geologie, Munich, Germany) (Fig. 1). Both specimens are large adults from the *Lystrosaurus* AZ of the Karoo Basin of South Africa (Ezcurra & Butler 2015b). The left side of SNSB-BSPG 1934 VIII 514 is nearly complete, but the right side has been subject to severe deformation and loss of information (Fig. 1B-C). The specimen also previously underwent substantial reconstruction in an attempt to adhere disarticulated and fractured elements, especially in the premaxillary region (Broili & Schröder 1934). RC 846 is far more complete but the skull is moderately transversely compressed and its posterior region has been moderately crushed. The premaxilla is also largely complete and articulated in this specimen.

Scanning

RC 846 was CT scanned at the University of Texas High-Resolution X-ray CT Facility Archive. The braincase of RC 846 is disarticulated from the rest of the skull, allowing it to be µCT scanned separately (hereafter 'RC 846 µCT'). SNSB-BSPG 1934 VIII 514 was CT scanned at the Klinikum rechts der Isar (Munich). Datasets consist of 548 coronal slices (1024 x 1024 pixels, voxel size 0.211 mm) for RC 846, 457 oblique (~15° ventroposterior deviation) coronal slices (1024 x 1024 pixels, voxel size 0.117 mm) for RC 846 µCT, and 1229 coronal slices (768 x 526 pixels, voxel size 0.5 mm) for SNSB-BSPG 1934 VIII 514. Original CT data for SNSB-BSPG 1934 VIII 514 are available in the Dryad Digital Repository: https://datadryad.org/review?doi=doi:10.5061/dryad.XXXX. Original CT data for RC 846 are archived at Yale University and are available from B.-A.S. upon request.

Virtual Endocast Construction

The CT data were imported into SPIERSedit (2.20, www.spiers-software.org). Areas of interest such as the endosseous labyrinths, braincase and nerves were manually segmented using the Masks and Curves tools following Balanoff *et al.* (2016) (see Brown *et al.* 2019, fig. S1). Interactive 3D PDFs of the endocranial reconstructions are provided as supplementary information.

Morphometric Outline Analysis

Elliptical Fourier analysis (EFA) was used in this study to quantify the morphological variability of brain and inner ear endocasts among diapsid groups. EFA statistically compares the co-ordinates of complex 2D shapes or outlines. EFA is very versatile as it can be used to compare shapes where homologous features are hard to distinguish (Crampton 1995). As a result, EFA is widely used in both the palaeontological and biological sciences to study interspecific (e.g. Crampton 1995; Bonhomme *et al.* 2013; Vidal *et al.* 2014; Lautenschlager 2014; Lautenschlager *et al.* 2018) and intraspecific (e.g. Polihronakis 2006; Ramajo *et al.* 2013) anatomical variation.

Brain Outline Preparation. An outline of the most complete *Proterosuchus fergusi* endocranial reconstruction (RC 846) was drawn in Adobe Illustrator (CS5, www.adobe.com). The brain cavities of 69 extinct and extant archosauriforms compiled from the literature were also outlined in Adobe Illustrator. For consistency, the left lateral view was always used. If unavailable, the right lateral view was reversed. Natural, artificial (e.g. latex) and virtual endocasts were used for comparative taxa. Brain cavity outlines and taxonomic information of all comparative taxa are available in Table S1. Outline co-ordinates were digitised in tpsDig2 (v2.31, Rohlf 2010) as 1000 x/y pairs.

Inner Ear Outline Preparation. The inner ear is divided into two regions, both with different functions: the semi-circular canals are part of the vestibular region, responsible for balance and co-ordination; whereas the endosseous cochlear duct (ECD) is part of the auditory system, responsible for hearing. To determine whether these features have evolved separately the inner ear was outlined and analysed both with and without the ECD. Analysis without the ECD also allowed the inclusion of the basal archosauriform *Euparkeria capensis,* for which the ECD could not be reconstructed (Sobral *et al.* 2016a). Prior to this study, *E. capensis* was the only non-archosaurian archosauriform for which three articulated semi-circular canals had been virtually reconstructed.

For this analysis, a computerised outline procedure was used. Images of the left labyrinth from extinct and extant diapsid taxa (n = 94, with ECD; n = 99, without ECD) were collected from the literature. These were then converted into binary images by altering the threshold in Adobe Photoshop (CS5, www.adobe.com). At this stage for the analysis excluding the ECD, the polygonal lasso tool was used to select and remove the ECD. Images were then vectorised using the 'Live Trace' tool in Adobe Illustrator before using the expand tool to make the vector editable. The 'Outline Stroke' tool was then used to create a computer-generated outline. All endosseous labyrinths were outlined in lateral view. If the left labyrinth was unavailable, the right labyrinth was reversed. Inner ear outlines and taxonomic information of all comparative taxa are available in the supplementary information. Co-ordinates for the outlines were digitised in tpsDig2 as 1000 x/y pairs for outlines with the ECD and 750 x/y pairs for outlines without the ECD.

Elliptical Fourier Analysis. Outline co-ordinates were analysed respectively in PAST (v3.19, Hammer *et al.* 2001) using EFA. Outlines were smoothed ten times to eliminate pixel noise, and 23 Fourier harmonics were found to describe the outlines of all sampled taxa sufficiently (average Fourier power > 99%). A Procrustes superimposition was performed before undergoing principal component analysis (PCA). Taxa were assigned to a phylogenetic group and broad ecological group (aquatic, semi-aquatic, terrestrial) (see Table S1). To test whether morphological variation was significantly different between group variables (ecological and phylogenetic) the non-parametric one-way PERMANOVA test was used with 10,000 permutations. Due to the ambiguity surrounding the ecology of *Proterosuchus fergusi*, this taxon was excluded from analyses between ecology.

Morphometric Landmark Analysis

This analysis is an iteration of that used by Yi & Norell (2015), Neenan *et al.* (2017) and Neenan *et al.* (2019) to compare the endosseous labyrinths of extant snakes, extinct sauropterygians and *Massospondylus* individuals, respectively. However, unlike those mentioned this analysis compares each of the different semi-circular canals (anterior semi-circular canal, ASC; lateral semi-circular canal, LSC; posterior semi-circular canal, PSC) separately.

The semi-circular canals generated from RC 846 µCT and RC 846 were used for this analysis. Additionally, the inner ears of comparative extinct and extant diapsid taxa (n=37, ASC; n=51, LSC; n=35, PSC) were sourced from the literature. The left labyrinth was selected for this analysis due to its relative availability, but if unavailable the right labyrinth was reversed.

Screenshots of each semi-circular canal were taken perpendicular to the plane to remove perspective skew. The external and internal surface of each canal was outlined in Adobe Illustrator using the automated approach described above. The dashed line stroke tool was used to find 21 equally-spaced points along the external surface of each canal and 11 along the inner surface of each canal. These dashed lines were used as a reference point for accurate and consistent landmark placing. The outlines with their reference points were imported into tpsDig2 and landmarks were placed in a designated order. Co-ordinates were exported from tpsDig2 and imported into MorphoJ (v1.06d, www.flywings.org.uk/morphoj_page.htm). To mitigate the effects of varying orientation, sizing, and distance between landmarks of different canals, a Procrustes superimposition was performed (following Neenan *et al.* 2017). Principal component analysis was run and plotted to show geometric variability. A canonical variate analysis (CVA) was used to test the morphological variance of diapsid semi-circular canals between different phylogenetic and ecologic groupings, respectively. Due to the ambiguity surrounding the ecology of *Proterosuchus fergusi*, this taxon was excluded from analyses between ecology.

Head posture

The orientation of the LSC ('horizontal semi-circular canal') has been widely used to infer the head posture of fossil taxa (Rogers 1998; Witmer *et al.* 2003; Sampson & Witmer 2007; Sereno *et al.* 2007; Witmer *et al.* 2008; Witmer & Ridgely 2009; Neenan & Scheyer 2012; Benoit *et al.* 2017), however not without criticism (Hullar 2006; Taylor *et al.* 2009; Marugán-Lobón *et al.* 2013). As part of the vestibular system, it is thought that many species habitually hold their LSC in a horizontal orientation (Lebedkin 1924; de Beer 1947). For example, the LSC orientation in the basal sauropterygian *Placodus gigas* suggests that it was down tilted

~20° (Neenan & Scheyer 2012). Neenan & Scheyer (2012) suggested that the downturned head posture was adapted for aquatic herbivory and concluded that *Pl. gigas* was fully adapted for aquatic life despite being one of the most basal sauropterygians.

Orientation of the lateral semi-circular canal. Screenshots of the isolated LSC and whole skull (skull at 75% opacity) were taken in SPIERS View to show both the skull and LSC. The orientation of each LSC was measured in ImageJ using the angle tool. Lateral semi-circular canals reconstructed from RC 846 μCT were excluded from this analysis because the scans only contained the braincase region. Often in these analyses, the 'horizontal' is measured as the bottom surface of the dentary (e.g. Witmer & Ridgely 2009). However, as both of the mandibles in RC 846 and SNSB-BSPG 1934 VIII 514 are significantly deformed, the maxillary tooth-line was used instead as the horizontal plane. The left and right LSC planes were measured separately. The mean average was calculated from all four values.

Auditory Abilities

The mean hearing frequency and hearing range of *Proterosuchus fergusi* were estimated following methods from Walsh *et al.* (2009). The endosseous cochlear duct (ECD) length is considered a proxy of auditory ability. The study from Walsh *et al.* (2009) used a linear regression of scaled ECD length and sensitivity data of extant avian and reptilian taxa to estimate the auditory abilities of several extinct Aves. This has since been repeated with the Early Jurassic marine crocodylomorph *Steneosaurus* cf. *gracilirostris* (Brusatte *et al.* 2016) and with the basal eusuchian *Lohuecosuchus megadontos* (Serrano-Martínez *et al.* 2018). As individuals can typically only hear within their own vocal range, estimations of auditory acuity can be informative regarding vocality (Narins *et al.* 2004). Vocality and auditory

ability are also considered to be indicators of sociality and cognitive ability, since larger more complex groups require better communicative skills to work together efficiently (Blumstein & Armitage 1997; Freeberg *et al.* 2012; Freeberg & Krams 2015; Sewall 2015). This is corroborated by Walsh *et al.* (2009) who found longer ECD length to be significantly correlated with animals living in larger group sizes.

Regressions. This study uses ECD length (scaled to basicranial length) and hearing sensitivity data derived from Walsh *et al.* (2009). Additional data on the hearing sensitivity of extant archosaurs was also collected from the literature (Corfield *et al.* 2013; Bonke *et al.* 2015) giving a total of 26 comparative taxa. RC 846 produced the most complete endocast and so was the only proterosuchid specimen used in the analysis. The ECD length of RC 846 was measured and scaled to the basicranial length (measured from the basisphenoid-presphenoid suture to the caudal-most tip of the occipital condyle, S. Walsh 2018 pers. comm.).

All scaled ECD lengths were log-transformed. Log-scaled ECD length for extant taxa was plotted against respective mean hearing and hearing range data. Both an ordinary least squares linear regression and a phylogenetic generalized least square regression were calculated for this analysis. These regression lines were used to predict mean hearing and hearing range for *Proterosuchus fergusi* based on the scaled and log-transformed ECD length. Analyses were conducted using R (RStudio v1.1.423, www.rstudio.com). The R packages ape (5.3, Paradis *et al.* 2004), geiger (2.0.6.1, Harmon *et al.* 2007), nlme (3.1-137, Pinheiro *et al.* 2018) and phytools (0.6-60, Revell 2012) were used to calculate the phylogenetic generalized least square (PGLS) regression with a Brownian motion model of trait evolution. The analysis used a phylogenetic tree of all comparative taxa generated from http://timetree.org/.

Snout Beam Analysis

Beam theory was used to investigate the relative rostral resistance of *Proterosuchus fergusi* to bending and torsion. Beam theory calculates the potential bending of an object based on the density and distribution of material around the neutral axis (the centre of an object, where there is no tension or compression) (Therrien *et al.* 2005; Cuff & Rayfield 2013). For example, a hollow tube is more resistant to bending than an infilled tube because material is distributed further from the neutral axis. To test the biomechanical resistance of rostra and lower jaws, this technique has been previously applied to a range of fossil taxa (Therrien *et al.* 2005; Cuff & Rayfield 2013; Foffa *et al.* 2014).

Slice Preparation. Slices were chosen along the rostrum at intervals. The first 20% of the rostrum was sliced at intervals of 2% as the premaxillary area is of specific interest in *Proterosuchus fergusi*. Due to the extent of the overhanging premaxilla in *P. fergusi*, a straight beam may not be considered appropriate for this taxon. Therefore, for the rostral 20% of the snout both a straight beam and curved beam were used in the analysis for *P. fergusi*. For the curved beam analysis, the rostrum of *P. fergusi* was sliced at intervals of 4% rather than 2% to prevent slices overlapping. The latter 80% of the rostrum was sliced at intervals of 10%. RC 846 was used for this analysis because the premaxillae of SNSB-BSPG 1934 VIII 514 have undergone significant reconstruction and may not represent the true original shape (Fig. 1). As RC 846 was scanned along the coronal axis, the raw CT slices could be used in this analysis.

For comparative analysis, five extant taxa were chosen: four pseudosuchians, *Alligator mississippiensis* (American alligator), *Crocodylus moreletii* (Morelet's crocodile), *Crocodylus rhombifer* (Cuban crocodile) and *Tomistoma schlegelii* (false gharial); and one

actinopterygian, *Atractosteus spatula* (alligator gar). *Atractosteus spatula* was included because of the slight overhang of the premaxilla, similar to that of *P. fergusi*.

The skull of *A. spatula* was downloaded as CT data from Digimorph.org. The specimen was scanned along the coronal plane so slices for this analysis could be taken directly from the raw CT-scans. Skulls of *C. moreletii*, *C. rhombifer*, and *T. schlegelii* were downloaded as STL files from Digimorph.org. *Alligator mississippiensis* (juvenile) was downloaded from Digimorph.org as CT data sliced along the horizontal plane so the raw slices could not be used in this analysis. *Alligator mississippiensis* was exported from SPIERSview as an STL file. These four STL files were imported into Blender (2.79a, www.blender.org) and manually sliced using the Boolean Modifier tool. A visual reference was used to accurately slice at the correct positions along the rostrum. All slices were rendered against the same flat plane for consistency. For the curved beam analysis RC 846 was imported into Avizo Lite (9, Thermo Fisher Scientific) and the rotate tool was used create the required slices.

All slices were imported into Adobe Photoshop where mandibles were manually removed. Teeth can vastly increase the proportion of material in the slice, especially in specimens with larger teeth (Cuff & Rayfield 2013). To standardise these effects, teeth were removed and the alveoli flattened in all slices. Additionally, in *P. fergusi*, the sediment was manually removed from the slices and rostrum walls were slightly corrected by symmetrisation. All slices were then converted into binary images by altering the image threshold.

Second moments calculation and analysis. Prepared slices were imported into ImageJ (1.51j8, www.imagej.nih.gov/ij). The second moments of area in the dorsoventral (Ix) and

mediolateral (Iy) directions and the polar moment of inertia (J) were calculated using the ImageJ macro, MomentMacroJ (v1.4, www.hopkinsmedicine.org/fae/mmacro.html). In an additional analysis, rostra were scaled to the rostral length of *Proterosuchus fergusi* (aspect ratio was maintained) to determine whether size difference influenced results (see Supplementary material). All results were log transformed and plotted using R. A paired t-test was computed between *P. fergusi* and comparative taxa for the entire rostrum and the first anterior 20% of the rostrum both at true size and scaled size and also using both a straight and curved beam.

RESULTS

Virtual Endocast Reconstruction

Brain Cavity. The endocranial reconstructions of *Proterosuchus fergusi* are generally linear in shape and organisation (Fig. 2), similar to that of modern-day adult crocodylians (Jirak & Janacek 2017). The brain cavity of *P. fergusi* is straighter than many archosauriforms including erythrosuchids (Gower & Sennikov 1996), phytosaurs (Holloway *et al.* 2013; Lautenschlager & Butler 2016) and many crocodylomorphs (Witmer *et al.* 2008; Witmer & Ridgely 2009; Kley *et al.* 2010), but analogous to the thalattosuchians *Pelagosaurus typus* and *Steneosaurus gracilirostris* (Brusatte *et al.* 2016; Pierce *et al.* 2017).

Due to breaks at the frontal-parietal suture in both RC 846 and SNSB-BSPG 1934 VIII 514, the elongate olfactory tracts typical of many archosauriforms and non-archosauriform diapsids (Witmer *et al.* 2008; Witmer & Ridgely 2009; Ezcurra 2014; Lautenschlager & Butler 2016; Trotteyn & Paulina-Carabajal 2016) could not be fully reconstructed in *P. fergusi*. The endocast for RC 846 μCT lacks the anterior portion of the

olfactory region, which would lie on the ventral surface of the frontals. This region is also missing in SNSB-BSPG 1934 VIII 514 due to the poor preservation of the frontals. Shallow concave fossae along the ventral surface of the frontals of RC 846 allow for the partial reconstruction of the dorsal surfaces of the olfactory bulbs (Fig. 2C-D). The ventral extent of the bulbs cannot be determined due to the lack of constraining bones in the region. The bulbs are slightly laterally expanded and rostrally taper out into two separate structures. Unlike in the basal archosauromorph *Tasmaniosaurus triassicus* (Ezcurra 2014), the olfactory bulbs of *P. fergusi* are exceeded in width by the cerebral hemispheres. The morphology of these bulbs allows for an estimation of the size and extent of the olfactory tracts and olfactory region as a whole. Compared to other archosauriforms the olfactory region is relatively short, analogous to the thalattosuchian *Pelagosaurus typus* (Pierce *et al*. 2016), but considerably larger than the ornithosuchid *Riojasuchus tenuisceps* (Baczko & Desojo 2016).

The forebrain is bulbous and horizontal while the mid-brain is more anteroventrally directed. The floccular lobes are relatively small and do not extend through the anterior semi-circular canal, unlike in many archosaurs (e.g. Witmer & Ridgely 2009; Lautenschlager *et al*. 2012; Lautenschlager & Butler 2016). The hind brain is mediolaterally narrow, especially between the endosseous labyrinths, but expands ventrally more than other parts of the braincase. Ventral to the hindbrain, pituitary fossae are partially preserved in both specimens, but not sufficiently to reconstruct. The main body of the brain cavity (forebrain-hindbrain) sits underneath the parietal and post-parietal bones.

The carotid artery canal could only be reconstructed in SNSB-BSPG 1934 VIII 514. The carotid canal extends ventrally from the braincase before dividing into two canals that then extend away from each other laterally. This is unlike the condition in many archosauriformes where the carotid artery extends out from the pituitary fossa (Witmer *et al.* 2008; Witmer & Ridgely 2009; Lautenschlager & Butler 2016). This suggests the pituitary is

considerably reduced in *P. fergusi* and projects posteriorly. A bony margin separating the pituitary from the diencephalon is not recognisable in the CT data.

A small ventrally positioned nerve canal reconstructed in SNSB-BSPG 1934 VII I 514 may be the trochlear nerve canal (iv). However, it does not sit rostrally to the trigeminal nerve (v) as occurs in phytosaurs (Lautenschlager & Butler, 2016). In RC 846 and SNSB-BSPG 1934 VIII 514 a group of nerves were reconstructed on the lateral surface of the endocast and may be the three branches of the trigeminal nerve canal (v). It seems to be in a position similar to the trigeminal nerve in thalattosuchians (Brusatte *et al.* 2016; Pierce *et al.* 2016) but more anteriorly positioned than in phytosaurs (Lautenschlager & Butler 2016). Similar reconstructions on RC 846 µCT were considered too dorsally positioned to be cranial nerves and so were identified as venous canals.

Anterior to the carotid artery canal on SNSB-BSPG 1934 VIII 514 is a small ventrolaterally-directed nerve canal, possibly the abducens nerve (vi). This nerve is also reconstructed in RC 846. In all of the reconstructions a cranial nerve sits immediately anterior to the endosseous labyrinths. This nerve is similar in position to what has been interpreted as the facial nerve (vii) in many extinct and extant archosauriforms (Gower & Sennikov 1996; Sampson & Witmer 2007; Witmer *et al.* 2008; Witmer & Ridgely 2009; Knoll *et al.* 2012; Lautenschlager *et al.* 2012; Lautenschlager *et al.* 2014; Lautenschlager & Butler 2016; Pierce *et al.* 2017). The ventral portion of the braincase of RC 846 is poorly preserved, limiting the reconstructions available. The endosseous labyrinths are relatively large in comparison to the braincase, making up on average 7.9% the volume of the brain cavity.

Inner Ear. The endosseous labyrinths of all three specimens were reconstructed completely (Fig. 3). The vestibular regions (top portion) of the endosseous labyrinths of *Proterosuchus*

fergusi have a pyramidal shape superficially comparable to the thalattosuchians *Steneosaurus gracilirostris* (Brusatte *et al.* 2016) and *Pelagosuchus typus* (Pierce *et al.* 2017). While in lateral view the anterior semi-circular canal (ASC) looks substantially larger than the posterior semi-circular canal (PSC), the canals are actually relatively equal in their proportions. This morphological feature is shared among many non-archosaurian archosauriformes and early pseudosuchians (Brusatte *et al.* 2016; Lautenschlager & Butler, 2016; Pierce *et al.* 2016; Sobral *et al.* 2016b) but is thought to be a plesiomorphic trait lost in extinct and extant crocodylomorphs, which tend to have considerably larger anterior canals compared to the posterior canal (Georgi & Sipla 2008; Witmer *et al.* 2008; Witmer & Ridgely 2009; Pierce *et al.* 2017). The ASC and LSC are elliptical in shape, whereas the PSC is straighter. The PSC of SNSB-BSPG 1934 VIII 514 has a pronounced ventrally-directed kink, unlike the condition in RC 846. This feature is more pronounced in the right PSC and therefore likely the result of post-mortem deformation of the specimen (Fig. 3C-D).

The endosseous cochlear duct (ECD) is significantly less ventrally extended than in other archosauriform reconstructions (e.g. Lautenschlager & Butler 2016; Brusatte *et al.* 2016; Pierce *et al.* 2017; Leahey *et al.* 2015; Witmer *et al.* 2008). The fenestra vestibuli (which connects the inner and middle ears) is visible in RC 846 and possibly in SNSB-BSPG 1934 VIII 514 and extends posterolaterally away from the labyrinth.

Morphometric Outline Analysis

Brain Outlines. EFA was used to compare the brain cavity endocast of *Proterosuchus fergusi* to that of various extant and extinct archosauriforms. As the olfactory bulbs are only reconstructed in RC 846, this endocast was outlined and analysed. The first three principal component (PC) axes (Fig. 4 & Brown *et al*. 2019, fig. S2-3) account for 79.2% of shape

variation. *Proterosuchus fergusi* and the proterochampsian *Tropidosuchus romeri* (the only other non-archosaurian archosauriform with an endocast sufficiently complete enough to be included in the analysis; Trotteyn & Paulina-Carabajal 2016) fall well within the non-phytosaur pseudosuchian morphospace in PC1 vs. PC2 (Fig. 4). Minimum spanning trees show that *P. fergusi* is placed closest to *Sebecus icaeorhinus* (early–mid Eocene sebecid crocodylomorph) and *Gavialis gangeticus* (gharial) in PC1 vs. PC2 (Brown *et al*. 2019, fig. S4) and PC1 vs. PC3 (Brown *et al*. 2019, fig. S5), respectively. Both PC plots show clear divisions between phylogenetic groups, with groups with similar ecological niches such as birds and pterosaurs, and phytosaurs and crocodylomorphs, overlapping each other in morphospace. PERMANOVA tests show significant differences between the endocranial morphology of semi-aquatic and terrestrial taxa in the analysis (Table 1) as well as significant support for the separation in morphospace of many groups within the clade Archosauriformes (Table 2).

Inner Ear Outlines. EFA was used to test the anatomical variations between the inner ears of diapsids, both with (w/) and without (w/o) the ECD. The first two PC axes account for 70.1% and 72.9% of shape variation with (Fig. 5A) and without the ECD (Fig. 5B), respectively. In both PC plots, RC 846 overlaps in morphospace with aquatic, semi-aquatic and terrestrial taxa. RC 846 μCT similarly lies within all three morphospaces when the ECD is excluded (Fig. 5B), but lies outside all morphospace when the ECD is included (Fig. 5A). Minimum spanning trees (Brown *et al*. 2019, fig. S7A & S7B) show that both RC 846 and RC 846 μCT lie closest to terrestrial squamates, with the exception of RC 846 μCT which comes out closest to the sauropodomorph *Antarctosaurus wichmannianus* when the ECD is excluded (Brown *et al*. 2019, fig. S7B).

Plots show substantial morphospace overlap between different ecological groupings. However, PERMANOVA tests (Table 3) show significant differences between the inner ear morphology of taxa from all ecologies when the ECD is included, and between aquatic taxa and both terrestrial ($p = 0.0013$) and semi-aquatic taxa ($p = 0.0282$) when excluded. Phylogenetic groupings are generally not very distinguishable in either iteration, but at higher taxonomic ranks 'archosauromorphs' and 'outgroup taxa' (testudines, sauropterygians and squamates) show a clear divergence when the ECD is included (Brown *et al*. 2019, fig. S8A) compared to when the ECD is excluded (Brown *et al*. 2019, fig. S8B). PERMANOVA tests (Table 4) show that when the ECD is included, basal archosauriforms (which includes solely *Proterosuchus fergusi* in this iteration) are significantly different to all groups apart from sauropterygians ($p= 0.2562$), testudines ($p= 0.1189$) and phytosaurs (0.0995). However, when the ECD is excluded, basal archosauriforms (which includes both *P. fergusi* and *Euparkeria capensis* in this iteration) are significantly different to fewer groups, including more derived archosauriform groups: Phytosauria ($p= 0.7363$), non-phytosaurian pseudosuchians ($p= 0.1340$) and sauropods ($p = 0.0618$).

Morphometric Landmark Analysis

The PC plots (Fig. 6) demonstrate the variation in the morphology of the semi-circular canals of diapsids based on landmarks. The three PC axes (Fig. 6A-C) account for 81.2%, 74.1% and 80.8% of shape variation across the ASC, LSC and PSC, respectively. CVA results (Table 5) support significant differences between ecological groupings in most cases, with terrestrial and aquatic taxa differing significantly across all semi-circular canals ($p= 0.0002$, ASC; $p= 0.0050$, LSC; $p= 0.0051$, PSC). RC 846 is recovered in morphospace occupied by terrestrial, semi-aquatic and aquatic taxa in ASC and LSC, but places outside occupied morphospace in

the PSC plot. Whereas RC 846 μCT is displaced from all occupied morphospace in both the PSC and LSC plots, but overlaps with aquatic taxa in the ASC plot (Fig. 6A). All three PC plots seem to separate taxa by phylogenetic group relatively well; however, CVA results show very few significant results between phylogenetic groupings (Table S2). Across all semi-circular canals, basal archosauriforms (solely *P. fergusi*) are only significantly different to Aves ($p= 0.0231$, ASC; $p= 0.0208$, LSC; $p= 0.0211$, PSC).

Head Posture

Relative to the horizontal, the average orientation of the LSC plane is 17.19° (Fig. 7A), suggesting *Proterosuchus fergusi* had a significantly upright 'alert' head posture (Fig. 7B). This is in contrast to *Crocodylus johnstoni* (freshwater crocodile), which has a horizontal head posture when the LSC plane is aligned to the horizon (Fig. 7C; Witmer *et al.* 2008).

Auditory Abilities

Both the linear and PGLS regression (Fig. 8; solid line and dashed line, respectively) support significant relationships between ECD length and both mean hearing and hearing range in extant taxa (Fig. 8). On the basis of these relationships, the auditory abilities of *Proterosuchus fergusi* have been estimated. Both regression lines reveal considerably different reconstructions, with the linear regression predicting a mean hearing frequency of ~525Hz and a hearing range of ~780Hz (similar to that of *Alligator mississippiensis* and the rhynchocephalian *Sphenodon punctatus*), and the PGLS regression predicting a mean hearing frequency of ~1275Hz and a hearing range of ~2150Hz (similar to that of the terrestrial squamate *Ptyodactylus hasselquistii*).

Snout Beam Analysis

Plots generally show similar trends in all taxa, with second moment and moment of inertia values generally increasing steadily posteriorly along the rostra (Fig. 9). Pertaining to the anterior 20% of the rostrum of *Proterosuchus fergusi*, differences between the straight and curved beam (Fig. 9, solid and dashed line, respectively) analysis are relatively consistent across all plots; with the straight beam showing a more posteriorly positioned peak (~15% along the rostrum length) compared to the curved beam (~4% along the rostrum length). *Tomistoma schlegelii* (false gharial) is the only comparative taxa that is significantly different to *P. fergusi* across all iterations of the analysis and all moments of resistance (Table S4).

Values of Ix, which represents resistance to dorsoventral bending, (Fig. 9A-B) are highest in *Proterosuchus fergusi*, even when other taxa are size-corrected. True size plots show that *Atractosteus spatula* (alligator gar) is the least resistant (Fig. 9A), but when scaled *Tomistoma schlegelii* is the least (Fig. 9B). Paired t-test results from the straight beam iteration show that there is no significant difference in resistance along the whole rostrum between *P. fergusi* and the crocodylids when scaled (Table S4), but it is worth noting that this is not the case when a curved beam is used instead.

Resistance to mediolateral bending (Iy) is very similar between *Proterosuchus fergusi* and the crocodylids when scaled (Fig. 9C) This is also demonstrated by the paired t-test results, which show no significant differences in Iy values between *P. fergusi* and the crocodylids at true size (Table S4). However, when taxa are size-corrected *P. fergusi* has relatively poor resistance compared to the other taxa (Fig. 9D).

Resistance to torsion (J) is the sum of Ix and Iy and so follows the general trends of Ix and Iy. *Proterosuchus fergusi* has J values very similar to *Crocodylus rhombifer* and

Crocodylus moreletii at true size (Fig. 9E; Table S4). When taxa are scaled, all species have very similar torsion resistance, except *T. schlegelii* which is much lower (Fig. 9F).

DISCUSSION

Life habits of Proterosuchus

Hearing. The lower portion of the inner ear contains the ECD, which comprises sound-detecting cells that are stimulated by sound waves transmitted from the middle ear (Sobral *et al.* 2016b). The virtual reconstruction of the ECD of *Proterosuchus fergusi* has permitted an estimation of the mean hearing frequency (MHF) and hearing range (HR). In order to understand the effects that phylogeny has on these interpretations, a PGLS regression was also used in addition to the linear regression proposed by Walsh *et al.* (2009). The regressions gave different results, with sensitivity range estimations of ~0.1–0.9 kHz and ~0.2–2.4 kHz for the linear and PGLS regressions, respectively. However, despite differences, results from both iterations concur that *P. fergusi* was probably more specialised to lower frequencies, much like modern crocodiles (Vergne *et al.* 2009; Walsh *et al.* 2009). Following the results of the linear regression, acoustic estimations for *P. fergusi* are on the lower end of sensitivity values known for modern crocodylians (Walsh *et al.* 2009), as well as the extinct crocodyliforms such as the thalattosuchian *Steneosaurus cf. gracilirostris* (Brusatte *et al.* 2015) and the basal euschian *Lohuecosuchus megadontos* (Serrano-Martínez *et al.* 2019), for which auditory acuity has also been estimated.

Estimations of auditory ability can also be informative in understanding the vocal complexity of a species. Considered to have resulted from coevolution of the vocal and auditory systems, individuals can typically only perceive frequencies within their own vocal

range (Narins *et al.* 2004). Vocality of a species can be used to infer behavioural aspects such as social complexity and ecology (Walsh *et al.* 2009; Walsh *et al.* 2014).

Sociality and vocality are integrally linked, with research suggesting social complexity has driven both vocal complexity and cognition in vertebrates (Blumstein & Armitage 1997; Freeberg *et al.* 2012; Freeberg & Krams 2015; Sewall 2015). Species that form larger and more complex social systems require a more complex vocal system to work together effectively. Therefore, vocal range, and thus auditory range, can be indicative of group size in a species. This is supported by results from Walsh *et al.* (2009) which found significant correlations between increased ECD length and larger social aggregations. Following this, the small ECD reconstructed in *P. fergusi* could suggest that it lived in small groups, or was even solitary.

In closed environments where visual communication is less effective (such as dense jungles), vocal and auditory complexity is highly advantageous (Garrick & Lang 1977; Brown & Waser 1984). In this study we find the relatively low acoustic complexity interpreted for *P. fergusi* to be consistent with the proposed absence of forests and vegetation following the Permo-Triassic mass extinction in the Karoo (Smith 1995; Ward *et al.* 2000; Smith *et al.* 2012). However, it is worth noting that while vocalisation and hearing ability in mammals is thought to be suggestive of habitat type (Brown & Waser 1984; de la Torre & Snowdon 2002), within living archosaur groups the relationship remains ambiguous (Garrick & Lang 1977; Nicholls & Goldizen 2006; Mason & Burns 2015).

Olfaction. The recognition of olfactory cues (sense of smell) is important for interspecific communication (e.g. kin recognition, finding a mate, territorial markers), navigation (e.g. foraging, predation, finding shelter and other resources), and avoiding dangers (e.g. predator

identification, poisonous food) (Dial & Schwenk 1996; Hemila & Reuter 2008; Krause *et al.* 2012; Müller *et al.* 2018). The olfactory bulbs, located anterior to the forebrain, contain olfactory receptor (OR) proteins that are responsible for detecting odorants (Freitag *et al.* 1998). The size of the olfactory bulbs generally corresponds to the quantity of OR proteins (Steiger *et al.* 2009), meaning that the enlargement of the olfactory bulbs is often indicative of increased olfactory abilities. Following this, the size of the olfactory bulbs has been widely used as a proxy for olfactory acuity in fossil taxa (Benton 1983; Brochu 2000; Kundrát 2007; Witmer *et al.* 2008; Witmer & Ridgely 2009; Zelenitsky *et al.* 2009; Bourke *et al.* 2014; Sales & Schultz 2014). The presence of olfactory fossae along the ventral surface of the frontals has allowed for the reconstruction of the olfactory bulbs in *Proterosuchus fergusi* (Fig. 2). The olfactory bulbs are analogous in relative size and shape to many modern crocodylians (Pritz 1975; Witmer *et al.* 2008; Jirak & Janacek 2017). Many crocodylians are considered to have a well-developed sense of smell, capable of quickly locating carrion both in the water and on land (Weldon *et al.* 1990). This suggests that proterosuchids may have had a similar olfactory acuity to modern crocodiles.

A latex endocast of *Tasmaniosaurus triassicus*, a sister-taxon to Archosauriformes (Ezcurra 2016) (previously considered a proterosuchid (Camp & Banks 1978)), revealed olfactory bulbs that were 1.4 times wider than the maximum width of the cerebrum (Ezcurra 2014). In *P. fergusi* the olfactory bulbs are only ~60% the maximum width of the cerebrum, suggesting significant differences in the life habits of these two Early Triassic carnivores. Ezcurra (2014) suggested the large olfactory bulbs in *T. triassicus* were indicative of a terrestrial ecology, following a study showing larger olfactory bulbs in fully terrestrial carnivorans in comparison to those with an aquatic affinity (Gittleman 1991). While the relationship between olfaction and habitat is more ambiguous in reptiles than mammals (Marek *et al.* 2015; Müller *et al.* 2018), the striking difference in relative olfactory width in

these two phylogenetically similar taxa suggests that *P. fergusi* may have been more adapted to aquatic environments than *T. triassicus*.

Prey Choice. Historically proterosuchids were considered aquatically-based predators, feeding on fish (Tatarinov 1961) and tetrapods, such as the dicynodont therapsid *Lystrosaurus* (Reig 1970). *Proterosuchus fergusi* occurs between 5–14 metres above the Permo-Triassic boundary in the lower levels of the *Lystrosaurus* AZ of the Karoo Basin (Smith & Botha-Brink 2014). During the deposition of these rocks there was a high abundance of potential prey items for *P. fergusi*, including dicynodont (e.g. *Lystrosaurus* spp.) and therocephalian (e.g. *Moschorhinus* and *Promoschorhynchus*) synapsids (Smith & Botha-Brink 2014). However, as no direct evidence of proterosuchid diet has been found (i.e. preserved gut contents), only indirect evidence such as tooth morphology and general anatomy can be used to infer feeding habit (Ezcurra *et al*. 2013).

Results of the rostral beam analysis show that the more oreinirostral morphology of *P. fergusi* was highly resistant to bending forces and torsion, comparable to the typically platyrostral morphology in *Crocodylus rhombifer* and *Crocodylus moreletii* (Fig. 9, Table S4). These results are consistent with finite element analyses from Rayfield & Milner (2008) comparing oreinirostral and platyrostral morphologies. The two *Crocodylus* species included in this analysis are generalists, feeding on a variety of prey items, including fish, amphibians, reptiles, birds and mammals (Platt *et al.* 2006; Milián-García *et al.* 2011). Juvenile and subadult crocodiles have an even more varied diet, with large quantities of invertebrates, gastropods and small vertebrates (Platt *et al.* 2006). Similarly, in *P. fergusi* the more gracile skull and relatively longer teeth of juvenile specimens has been thought to suggest that different ontogenetic stages favoured different prey items, possibly to decrease intraspecific

competition (Ezcurra & Butler 2015b). *Proterosuchus fergusi* may have had a generalist diet like modern crocodylians that change their diet through ontogeny from largely invertebrates to large terrestrial vertebrates. *Proterosuchus fergusi* and the platyrostral crocodylians (*Alligator mississippiensis*, *C. rhombifer*, *C. moreletii*) show significant differences in bending resistance to the longirostrine false gharial (*Tomistoma schlegelii*) in the analyses (Fig. 9, Table S4). This difference reflects the more specialist life habit of *T. schlegelii* with a predominately piscivorous diet (Pierce *et al.* 2008).

Ecological adaptations. Despite the presence of eleven well preserved specimens of *Proterosuchus fergusi*, there is currently no consensus on their ecology, or on the ecology of proterosuchids as a whole (Ezcurra *et al*. 2013). Original interpretations of a semi-aquatic habit for *P. fergusi* were in part due to the supposedly wet climate and palustrine environments presumed of the *Lystrosaurus* AZ. However, recent studies have shown that the Karoo Basin at this time was drastically different. Sedimentological analyses show the region was predominately semi-arid with vast braided rivers resulting from lack of vegetation (Smith 1995; Ward *et al.* 2000; Smith *et al.* 2012) and the climate fluctuated between droughts, sporadic flood events and extreme cold snaps (Smith 1995; Smith & Ward 2001; Viglietti *et al.* 2013; Smith & Botha-Brink 2014).

Endocranial reconstructions of the two *P. fergusi* specimens have not allowed us to make sound interpretations of its ecology based on palaeoneurology. Statistical tests of the brain cavity outline morphology (Table 1) show significant differences only between terrestrial and semi-aquatic taxa. This difference however is likely explained by the evolutionary divergence between predominately terrestrial avemetatarsalians and predominately semi-aquatic pseudosuchians. Similar morphometric analyses on the

endosseous labyrinth of saurians (Fig. 5) better separate groups based on ecology (Table 3), but also seem to be highly constrained by phylogeny (Table 4). The landmark-based analysis on individual semi-circular canals (Fig. 6) appears to be more appropriate for looking at ecology; statistical analyses show significant differences between the majority of ecological groupings (Table 5) and comparatively poor separation of phylogenetic groupings (Table S2). Across all three canals, *P. fergusi* resides consistently close to predominately semi-aquatic and aquatic taxa from various phylogenetically-distant groups (particularly sauropterygians, squamates and pseudosuchians). While the relationships between ecology, locomotion and function of a taxon and the endocranial anatomy are currently uncertain, several studies have recently attempted to elucidate this by looking at the morphology of the endosseous labyrinths (Cuthbertson *et al.* 2015; Yi & Norell 2015; Benson *et al.* 2017; Neenan *et al*. 2017). Based on our results, the endosseous labyrinths seem to be most appropriate for this type of analysis, particularly when individual semi-circular canals are separately analysed. If morphological differences are found to be indicative of ecological variation, with endosseous labyrinths comparable to various amphibious taxa, it is reasonable to postulate that *P. fergusi* may have had the sensory and balance organs required for semi-aquatic life.

In life, the endosseous labyrinths (semi-circular canals) are part of the vestibular system, responsible for balance and co-ordination. Endolymph fluid moves back and forth through each of the canals as the skull rotates, triggering receptors at the end of the canals that send signals to the brain (Clack 2016). Unlike the auditory organs, the function of these vestibular organs has largely remained constant over vertebrate evolution (Carey & Amin 2006) allowing extant animals to be used as analogues to inform about the balance of early tetrapods. For nearly a century many tetrapods have been thought to habitually hold the lateral semi-circular canal (LSC, or sometimes ‘horizontal semi-circular canal’) horizontally (Lebedkin 1924; de Beer 1947; Duijm 1951). Following this, over the last two decades the

LSC has been widely used to infer the head posture (typically 'alert' or 'resting') of various fossil groups (Rogers 1998; Witmer *et al.* 2003; Sampson & Witmer 2007; Sereno *et al.* 2007; Witmer *et al.* 2008; Witmer & Ridgely 2009; Neenan & Scheyer 2012; Benoit *et al.* 2017). The average orientation of the LSC in *P. fergusi* specimens SNSB-BSPG 1934 VIII 514 and RC 846 reconstructed in this study was ~17° (Fig. 7A), suggesting *P. fergusi* held its head tilted upwards (Fig. 7B). Among the array of taxa for which head posture has been inferred in this way, up tilted expressions are generally uncommon, especially to the degree found in *P. fergusi* (Marugán-Lobón *et al.* 2013). While the use of the LSC in inferring head posture has been met with scepticism, due to variation of inferred head postures found within phylogenetically similar groups (Hullar 2006; Taylor *et al.* 2009; Marugán-Lobón *et al.* 2013), several studies have suggested a possible relationship between the LSC and the resulting head posture linked to ecological factors (e.g. diet, feeding behaviour) and supported by osteological correlates (i.e. occipital position) (Sereno *et al.* 2007; Neenan & Scheyer 2012; Schellhorn 2018). If LSC orientation does show a behavioural and/or ecological signal, the range of LSC orientations recorded in the two specimens of *P. fergusi* indicate an upturned head posture and could be interpreted as an adaption to semi-aquatic life. When upturned ~17° the bones of the cranial roof lie almost horizontally and the vertically positioned external nares are about level with orbit height. When in the water, *P. fergusi* would be able to keep its eyes and nostrils out of the water while keeping a low profile close to the waterline with the rest of its body remaining fully submerged, alike to modern day crocodiles. As previously discussed, dorsally-positioned external nares are an adaptation to aquatic and semi-aquatic life that has convergently evolved in numerous groups over vertebrate evolution. Perhaps the upturned head posture of *P. fergusi* represents an alternative secondary adaptation for a semi-aquatic lifestyle among early diapsids. This would concur with the upwards tilting skull of *Lystrosaurus* (Benoit *et al.* 2017), which were

contemporaneous to proterosuchids and have likewise also been interpreted as possibly semi-aquatic (Retallack *et al.* 2003; Ray *et al.* 2005).

Functional morphology of the premaxilla

The overhanging premaxilla that characterises proterosuchids is enigmatic in origin and function. While unique in its accentuation, the snout morphology is analogous with several extant and extinct vertebrate groups. Within the clade Archosauriformes, ornithosuchids such as *Riojasuchus* and *Ornithosuchus* exhibit a superficially similar snout morphology to *Proterosuchus*. However, the comparatively few specimens known for ornithosuchids mean that limited information can be obtained about the functional morphology and evolution of this trait within archosauriforms. Modern analogues allow for the study of functional and sexual dimorphic aspects of this bizarre snout morphology. While phylogenetically distant, actinopterygians including *Oncorhynchus kisutch* (coho salmon) (Ezcurra 2017) and (to a lesser extent) many lepisosteids (gar) have a downturned premaxilla that does not fully occlude with the lower jaw. In *O. kisutch*, this trait is sexually selected for and found only in the hooknose adult male morphotype of the species (Fleming & Gross 1994). By contrast, in lepisosteids, this trait is thought to be functional in predation, for manipulating prey following capture (Lauder & Norton 1980).

Convergent features in fossil and living taxa have long been interpreted as inferring shared function, even between highly phylogenetically-distant groups (e.g. Ji *et al.* 2006; Field *et al.* 2011; O'Brien *et al.* 2016; Vullo *et al.* 2016; Arbour & Zanno 2019). Vullo *et al.* 2016 commented on the morphological similarities between the jaws of spinosaurid dinosaurs and an extant group of anguilliform fish (pike conger eels) and suggested that this inferred shared feeding behaviours. The lepisosteid *Atractosteus spatula* (alligator gar) was among

comparative taxa analysed for rostral resistance because of its overhanging premaxilla. Albeit far less accentuated compared to *Proterosuchus fergusi*, comparing results between the two overhanging premaxillae may have identified signals unique to this trait. The various statistical analyses tend to show significant differences between *P. fergusi* and *A. spatula* (Table S4). These results may suggest that *P. fergusi* did not share a similar method of predation to lepisosteids.

Growing and maintaining an oversized premaxilla with up to 18 ankylothecodont (deeply rooted and fused to the bone) teeth that would undergo periodic replacement, made the snout a costly phenotype (Ezcurra 2017). As such, without a morphological function, this trait would likely been negatively selected out of the population by natural selection (Andersson 1994). To date no physiological function has been suggested and mechanical functions such as digging have been ruled out after macroscopic analysis on the premaxillary teeth (Ezcurra 2017). The ontogenetic changes in the snout morphology (Ezcurra & Butler 2015b) and phenotypic costliness led Ezcurra (2017) to propose social and sexual selection as a possible explanation.

Snout beam analyses suggest that the premaxilla of *P. fergusi* is considerably resistant to dorsoventral bending and torsion compared to the crocodylians (Fig. 9; Table S4). The overhanging premaxilla does not seem to enhance or reduce resistance to mediolateral bending. The high resistance of the premaxilla to dorsoventral bending may be an indication of a specialist predation method. If this specialist function was beneficial enough it would outweigh the costliness of the premaxilla. However advanced biomechanical analyses such as finite element analysis would be required to test this hypothesis. It is possible that this phenotype may have been positively selected for under sexual selection, with a larger overhanging premaxilla being a signal for increased physical strength. While presumably sexual dimorphism was as widespread among fossil saurians as it is today, recognising sexual

dimorphism and even distinguishing gender is extremely difficult and problematic in the saurian fossil record (Bonnan *et al.* 2008; Ezcurra 2017; Mallon 2017). One aspect of sexual selection that could possibly be ruled out is the 'handicap principle' proposed by Zahavi (1975). The handicap principle states that survival of an individual to sexual maturity with a 'handicap' (in this instance the costly overhanging premaxilla) is evidence of overall fitness and therefore a suitable mate (Zahavi 1975; 1977). Resistance tests show that the premaxilla is not detrimental to rostral strength, therefore it is likely not a 'handicap' and this might not be a viable explanation of the phenotype.

Implications for the evolution of Archosauriformes

Evolution of the archosauriform brain. The endocasts of *Proterosuchus fergusi* reconstructed in this study are important contributions to understanding the evolution of basal archosauriform neuroanatomy (Fig. 10). While the palaeoneurology of archosaurian clades (particularly Dinosauria) have been extensively studied, stem archosaurs have been widely overlooked. Prior to this study, the endocranial anatomy of only three specimens of non-archosaurian archosauriform had been virtually reconstructed (Trotteyn & Paulina-Carabajal 2016; Fabbri *et al.* 2017) to add to the small number of informative artificial endocasts (Benton 1983; Gower & Sennikov 1996; Wharton 2000). Trotteyn & Paulina-Carabajal (2016) reconstructed the endocranium of the proterochampsian *Tropidosuchus romeri,* while Fabbri *et al.* (2017) reconstructed the endocranium of *P. fergusi* (RC 846 – although Fabbri *et al.* incorrectly identified the specimen as 'RC 96' which actually corresponds to a dicynodont (Ezcurra 2015)) and *E. capensis*. However, the endocasts from Fabbri *et al.* (2017) are incompletely figured and not described in the text and are therefore largely uninformative in regard to the morphology of the early archosauriform brain cavity.

Results of the morphometric analysis show that convergence in brain morphology has occurred multiple times in the archosauriform lineage, particularly in groups with similar life habits. A clear example of this is the significant overlap between bird and pterosaur brain morphology, both of which share a volant mode of life. These analyses also highlight similarities between the brain cavities of pseudosuchians and basal archosauriforms, especially when compared to avemetatarsalians. In some archosauriform groups (particularly non-avian theropods and avialans), endocranial morphology has been tentatively linked to orbit size, locomotion, ecology and organisation of cranial elements (Bhullar *et al.* 2012; Kawabe *et al.* 2013; Balanoff & Bever 2017; Fabbri *et al.* 2017). Perhaps with further research the correlations between form and function of the endocranial anatomy will become better understood and explain some of the similarities between relatively phylogenetically-distant taxa that our study displays.

Evolution of the archosauriform inner ear. The functional morphology and early evolution of the endosseous labyrinth is important for understanding the rise of archosaurs in the Mesozoic. Prior to this study no non-archosaurian archosauriform inner ear had been completely reconstructed (Fig. 11), leaving a significant gap in our understanding of how the vestibular and auditory systems have evolved in stem archosaurs.

In many eusuchians, the ASC is significantly longer compared to the PSC (Georgi & Sipla 2008; Witmer *et al.* 2008; Brusatte *et al.* 2016; Pierce *et al.* 2017). However, in more basal archosauriforms, the ASC and PSC are much more equal in size (Kley *et al.* 2010; Brusatte *et al.* 2016; Lautenschlager & Butler 2016; Sobral *et al.* 2016b; Pierce *et al.* 2017). Pierce *et al.* (2017) proposed that more equally proportioned anterior and posterior canals are plesiomorphic for Archosauriformes. The relatively equal size of the ASC and PSC in the

endosseous labyrinths reconstructed for *P. fergusi* is consistent with these interpretations. The relatively equal size of the ASC and PSC in phytosaurs has been suggested to be indicative of limited neck movement and semi-aquatic habitat (Sobral & Müller 2017). However, this seems unlikely as extant crocodiles inhabit semi-aquatic ecosystems and have relatively limited neck movements. Further research is required to determine the functionality of this derived trait in eusuchians.

The inner ears of archosaurs are significantly different to those of other diapsid groups. One of the most striking differences is the comparatively long ECD possessed by both crocodile-line and bird-line archosaurs. This trait seems to be confined to archosaurs, with most diapsid groups outside of Archosauromorpha (e.g. squamates, rhynchocephalians, testudines and sauropterygians) having relatively short cochlear ducts. Pierce *et al.* (2017) suggested that within Pseudosuchia the elongated cochlear duct evolved crownward to phytosaurs due to the small ECD present in the phytosaurs *Ebrachosuchus* and *Parasuchus* reconstructed by Lautenschlager & Butler (2016). However, Lautenschlager & Butler (2016) stated that the two phytosaur specimens were dorsoventrally compressed by ~40% and so the raw endocasts are not representative of true scale. When retrodeformed (Fig. 11E-F) the cochlear ducts are superficially and morphometrically similar to other pseudosuchians (Fig. 5A). Following this, the presence of the derived cochlear trait in both crocodile-line and bird-line archosaurs suggests the evolution of the trait occurred before Avemetatarsalia and Pseudosuchia diverged. However, prior to this study, the lack of labyrinth reconstructions in stem archosaurs meant that the origin of this trait could not be further constrained.

Reconstructions of the endosseous labyrinth reveal *P. fergusi* to have a relatively small ECD compared to crown archosaurs (Fig. 2; Fig. 11B). Morphometric analyses of the inner ear place *P. fergusi* close to non-archosaurian diapsids when the ECD is included, suggesting that the small ECD is a plesiomorphic trait (Fig. 5A). Following this it could be

postulated that the elongated ECD first evolved in archosauromorphs crownward of *P. fergusi*. As *P. fergusi* is the most basal member of the clade Archosauriformes (Nesbitt 2011), the most parsimonious inference is that a small cochlear duct is a plesiomorphic trait found in basal diapsids and retained in lepidosauromorphs and basal archosauromorphs. Subsequently, the derived trait of an elongate duct evolved somewhere in stem archosaurs and was retained in both avemetatarsalians and pseudosuchians. As a ventrally-extended ECD has been linked to increased auditory acuity (as previously discussed), perhaps the evolution of this derived trait marked a significant increase in auditory ability, vocality, sociality and cognition, all of which are thought to be integrally linked (Blumstein & Armitage 1997; Freeberg *et al.* 2012; Freeberg & Krams 2015; Sewall 2015). These developments may potentially have contributed to the radiation of archosaurs during the Triassic and Early Jurassic.

CONCLUSIONS

This study presents the first in-depth assessment of the braincase and inner ear of the Early Triassic basal archosauriform *Proterosuchus fergusi*. Morphological comparisons of endocranial reconstructions, supplemented by analyses on the skull posture, rigidity and auditory abilities, have revealed much about the probable life habits of *P. fergusi* and the evolution of the brain and inner ear through early archosauriform evolution. Endocranial reconstructions reveal *P. fergusi* had: (1) an endocranial cavity with low-angle brain flexures; (2) medium-sized olfactory bulbs; (3) pyramidal and sub-equally-sized semi-circular canals; (4) a small cochlear duct.

The brain morphology of *P. fergusi* is superficially and statistically similar to modern crocodylians and phytosaurs, and different to birds, pterosaurs and non-avian theropods. Assessment of the endocranial anatomy suggests that *P. fergusi* is estimated to be specialised

to lower frequency sounds, with a proficient sense of smell, both comparable to modern crocodiles. *Proterosuchus fergusi* held its head upwards ~17°, perhaps representing an alternative adaptation to semi-aquatic life than dorsally-positioned nares and orbits. The overhanging premaxilla remains largely enigmatic; with beam theory analyses indicating that generally this unusual morphology neither strengthens or weakens the snout and therefore purely non-functional selection pressures for this trait may be ruled out.

The small ECD of *P. fergusi* suggests basal archosauromorphs retained an ancestrally small ECD which later evolved to become elongate in more derived archosauriforms, before the divergence of avemetarsalians and pseudosuchians. The increase in auditory complexity as a result of an elongated ECD may indicate the coevolution of increased cognitive abilities, vocality and sociality in stem archosaurs, which could in turn have contributed to the radiation of archosaurs in the Triassic, forging the way for dinosaurs to dominate global faunas during the Mesozoic.

ACKNOWLEDGEMENTS

We thank Bruce Rubidge and Oliver Rauhut for access to specimens analysed in this study, and two anonymous reviewers for helpful comments and suggestions. This research was originally completed as EEB's MSci research in Palaeobiology & Palaeoenvironments at the University of Birmingham.

REFERENCES

ALLEMAND, R., BOISTEL, R., DAGHFOUS, G., BLANCHET, Z., CORNETTE, R., BARDET, N., VINCENT, P. and HOUSSAVE, A. 2017. Comparative morphology of snake (Squamata) endocasts: evidence of phylogenetic and ecological signals. *Journal of Anatomy*, **231**, 849–868.

ANDERSSON, M. 1994. *Sexual Selection*, Princeton University Press, 624 pp.

ARBOUR, V. M. and ZANNO, L. E. 2019. Tail Weaponry in Ankylosaurs and Glyptodonts: An Example of a Rare but Strongly Convergent Phenotype. *The Anatomical Record*. doi.org/10.1002/ar.24093

BACZKO, M. B. VON and DESOJO, J. B. 2016. Cranial anatomy and palaeoneurology of the archosaur *Riojasuchus tenuisceps* from the Los Colorados Formation, La Rioja, Argentina. *PLoS ONE*, **11,** e0148575.

BALANOFF, A. M., BEVER, G. S., COLBERT, M. W., CLARKE, J. A., FIELD, D. J., GIGNAC, P. M., KSEPKA, D. T., RIDGELY, R. C., SMITH, N. A., TORRES, C. R. and WALSH, S. 2016. Best practices for digitally constructing endocranial casts: examples from birds and their dinosaurian relatives. *Journal of Anatomy*, **229**, 173–190.

BALANOFF, A. M. and BEVER, G. S. 2017. The Role of Endocasts in the Study of Brain Evolution. 223-241. *In* KAAS, J. (ed.). *Evolution of Nervous Systems (2nd edition)*. Academic Press, 2007 pp.

BENOIT, J., MANGER, P. R., FERNANDEZ, V. and RUBIDGE, B. S. 2017. The bony labyrinth of late Permian Biarmosuchia: palaeobiology and diversity in non-mammalian Therapsida. *Palaeontologia africana*, **52**, 58–77.

BENSON, R. B., STARMER-JONES, E., CLOSE, R. A. and WALSH, S. A. 2017. Comparative analysis of vestibular ecomorphology in birds. *Journal of Anatomy*, **231**, 990-1018.

BENTON, M. J. 1983. The Triassic reptile *Hyperodapedon* from Elgin: functional morphology and relationships. *Philosophical Transactions of the Royal Society of London. Series B, Biological Sciences*, **302**, 605–718.

BENTON, M. J. and TWITCHETT, R. J. 2003. How to kill (almost) all life: the end-Permian extinction event. *Trends in Ecology & Evolution*, **18**, 358–365.

BHULLAR, B. A. S., MARUGÁN-LOBÓN, J., RACIMO, F., BEVER, G. S., ROWE, T. B., NORELL, M. A. and ABZHANOV, A. 2012. Birds have paedomorphic dinosaur skulls. *Nature*, **487**, 223.

BLUMSTEIN, D. T. and ARMITAGE, K. B. 1997. Does sociality drive the evolution of communicative complexity? A comparative test with ground-dwelling sciurid alarm calls. *The American Naturalist*, **150**, 179–200.

BONHOMME, V., PRASAD, S. and GAUCHEREL, C. 2013. Intraspecific variability of pollen morphology as revealed by elliptic Fourier analysis. *Plant Systematics and Evolution*, **299**, 811–816.

BONKE, R., WHITAKER, N., ROEDDER, D. and BOEHME, W. 2015. Vocalizations in two rare crocodilian species: A comparative analysis of distress calls of *Tomistoma schlegelii* (Müller, 1838) and *Gavialis gangeticus* (Gmelin, 1789). *North-Western Journal of Zoology*, **11**, 151–162.

BONNAN, M. F., FARLOW, J. O. and MASTERS, S. L. 2008. Using linear and geometric morphometrics to detect intraspecific variability and sexual dimorphism in femoral shape

in *Alligator mississippiensis* and its implications for sexing fossil archosaurs. *Journal of Vertebrate Paleontology*, **28**, 422–431.

BOTHA-BRINK, J. and SMITH, R. M. 2011. Osteohistology of the Triassic archosauromorphs *Prolacerta*, *Proterosuchus*, *Euparkeria*, and *Erythrosuchus* from the Karoo Basin of South Africa. *Journal of Vertebrate Paleontology*, **31**, 1238–1254.

BOURKE, J. M., RUGER PORTER, W. M., RIDGELY, R. C., LYSON, T. R., SCHACHNER, E. R., BELL, P. R. and WITMER, L. M. 2014. Breathing life into dinosaurs: tackling challenges of soft-tissue restoration and nasal airflow in extinct species. *The Anatomical Record*, **297**, 2148–2186.

BROCHU, C. A. 2000. A digitally-rendered endocast for *Tyrannosaurus rex*. *Journal of Vertebrate Paleontology*, **20**, 1–6.

BROILI, F. and SCHRÖDER, J. 1934. Beobachtungen an Wirbeltieren der Karroo Formation. V. Über *Chasmatosaurus vanhoepeni* Haughton. *Sitzungsberichte der Bayerischen Akademie der Wissenschaften, Mathematisch-Naturwissenschaftliche Abteiliung*, **3**, 225–264.

BROOM, R. 1903. On a new reptile (*Proterosuchus fergusi*) from the Karroo beds of Tarkastad, South Africa. *Annals of the South African Museum*, **4**, 159–164.

BROWN, C. H. and WASER, P. M. 1984. Hearing and communication in blue monkeys (*Cercopithecus mitis*). *Animal Behaviour*, **32**, 66–75.

BROWN, E. E., BUTLER, R. J., EZCURRA, M. D., BHULLAR, A.-B. and LAUTENSCHLAGER, S. 2019. Endocranial anatomy and life habits of the Early Triassic archosauriform *Proterosuchus fergusi*. *Dryad Digital Repository*. https://datadryad.org/review?doi=doi:10.5061/dryad.XXXX

BRUSATTE, S. L., MUIR, A., YOUNG, M. T., WALSH, S., STEEL, L. and WITMER, L. M. 2016. The braincase and neurosensory anatomy of an Early Jurassic marine crocodylomorph: implications for crocodylian sinus evolution and sensory transitions. *The Anatomical Record*, **299**, 1511–1530.

BUTTON, D. J., LLOYD, G. T., EZCURRA, M. D. and BUTLER, R. J. 2017. Mass extinctions drove increased global faunal cosmopolitanism on the supercontinent Pangaea. *Nature Communications*, **8**, 733.

CAMP, C. L. and BANKS, M. R. 1978. A proterosuchian reptile from the Early Triassic of Tasmania. *Alcheringa*, **2**, 143–158.

CAREY, J. and AMIN, N. 2006. Evolutionary changes in the cochlea and labyrinth: solving the problem of sound transmission to the balance organs of the inner ear. *The Anatomical Record*, **288**, 482–490.

CHEN, Z. Q. and BENTON, M. J. 2012. The timing and pattern of biotic recovery following the end-Permian mass extinction. *Nature Geoscience*, **5**, 375–383.

CLACK, J. A. 2016. Vertebrate diversity in a sensory system: the fossil record of otic evolution. 1–16. *In* CLACK, J. A., FAY, R. R., POPPER, A. N. (eds). *Evolution of the vertebrate ear*. Springer, 355 pp.

CORFIELD, J. R., KUBKE, M. F. and KÖPPL, C. 2013. Emu and kiwi: the ear and hearing in Paleognathous birds. 263–287. *In* KÖPPL, C., MANLEY, G. A., POPPER, A. N. and FAY, R. R. (eds). *Insights from comparative hearing research.* Springer, 388 pp.

CRAMPTON, J.S. 1995. Elliptic Fourier shape analysis of fossil bivalves: some practical considerations. *Lethaia*, **28**, 179–186.

CRUICKSHANK, A. R. I. 1972. The proterosuchian thecodonts. 89–119. *In* JOYSEY, K. A. and KEMP, T. S. (eds). *Studies in vertebrate evolution*. Oliver and Boyd, Edinburgh, 284 pp.

CUFF, A. R. and RAYFIELD, E. J. 2013. Feeding mechanics in spinosaurid theropods and extant crocodilians. *PLoS ONE*, **8**, e65295.

CUTHBERTSON, R. S., MADDIN, H. C., HOLMES, R. B. and ANDERSON, J. S. 2015. The braincase and endosseous labyrinth of *Plioplatecarpus peckensis* (Mosasauridae, Plioplatecarpinae), with functional implications for locomotor behavior. *The Anatomical Record*, **298**, 1597-1611.

DE LA TORRE, S. and SNOWDON, C. T. 2002. Environmental correlates of vocal communication of wild pygmy marmosets, *Cebuella pygmaea*. *Animal Behaviour*, **63**, 847–856.

DIAL, B. E. and SCHWENK, K. 1996. Olfaction and predator detection in *Coleonyx brevis* (Squamata: Eublepharidae), with comments on the functional significance of buccal pulsing in geckos. *Journal of Experimental Zoology*, **276**, 415–424.

DUIJM, M. J. 1951. On the head posture in birds and its relation features. *Proceedings of the Koninklijke Nederlandse Akademie van Wetenschappen C*, **54**, 202–271.

EZCURRA, M. D. 2014. The osteology of the basal archosauromorph *Tasmaniosaurus triassicus* from the Lower Triassic of Tasmania, Australia. *PLoS ONE*, **9**, e86864.

EZCURRA, M. D. 2015. *Systematics and evolutionary history of proterosuchian archosauriforms*. PhD thesis, University of Birmingham, UK.

EZCURRA, M. D. 2016. The phylogenetic relationships of basal archosauromorphs, with an emphasis on the systematics of proterosuchian archosauriforms. *PeerJ*, **4**, e1778.

EZCURRA, M. D. 2017. Can social and sexual selection explain the bizarre snout of proterosuchid archosauriforms?. *Historical Biology*, **29**, 348–358.

EZCURRA, M. D. and BUTLER, R. J. 2015a. Taxonomy of the proterosuchid archosauriforms (Diapsida: Archosauromorpha) from the earliest Triassic of South Africa, and implications for the early archosauriform radiation. *Palaeontology*, **58**, 141–170.

EZCURRA, M. D. and BUTLER, R. J. 2015b. Post-hatchling cranial ontogeny in the Early Triassic diapsid reptile *Proterosuchus fergusi*. *Journal of Anatomy*, **226**, 387–402.

EZCURRA, M. D. and BUTLER, R. J. 2018. The rise of the ruling reptiles and ecosystem recovery from the Permo-Triassic mass extinction. *Proceedings of the Royal Society B*, **285**, 20180361.

EZCURRA, M. D., BUTLER, R. J. and GOWER D. J. 2013. 'Proterosuchia': the origin and early history of Archosauriformes. 9–33. *In* NESBITT S. J., DESOJO, J. B., IRMIS, R. B., (eds). *Phylogeny and palaeobiology of early archosaurs and their kin*. Geological Society of London Special Publication, 379 pp.

EZCURRA, M. D., SCHEYER, T. M. and BUTLER, R. J. 2014. The origin and early evolution of Sauria: reassessing the Permian saurian fossil record and the timing of the crocodile-lizard divergence. *PLoS ONE*, **9**, e89165.

FABBRI, M., KOCH, N. M., PRITCHARD, A. C., HANSON, M., HOFFMAN, E., BEVER, G. S., BALANOFF, A. M., MORRIS, Z. S., FIELD, D. J., CAMACHO, J., ROWE, T.B., NORELL, M. A., SMITH, R. M., ABZHANOV, A. and BHULLAR, B. S. 2017. The skull roof tracks the brain during the evolution and development of reptiles including birds. *Nature Ecology & Evolution*, **1**, 1543.

FIELD, D. J., LIN, S. C., BEN-ZVI, M., GOLDBOGEN, J. A. and SHADWICK, R. E. 2011. Convergent evolution driven by similar feeding mechanics in balaenopterid whales and pelicans. *The Anatomical Record*, **294**, 1273-1282.

FLEMING, I. and GROSS, M. R. 1994. Breeding Competition in a Pacific Salmon (Coho: *Oncorhynchus kisutch*): Measures of Natural and Sexual Selection. *Evolution,* **48**, 637-657.

FOFFA, D., CUFF, A. R., SASSOON, J., RAYFIELD, E. J., MAVROGORDATO, M. N. and BENTON, M. J. 2014. Functional anatomy and feeding biomechanics of a giant Upper Jurassic pliosaur (Reptilia: Sauropterygia) from Weymouth Bay, Dorset, UK. *Journal of Anatomy*, **225**, 209-219.

FOTH, C., EZCURRA, M. D., SOOKIAS, R. B., BRUSATTE, S. L. and BUTLER, R. J. 2016. Unappreciated diversification of stem archosaurs during the Middle Triassic predated the dominance of dinosaurs. *BMC Evolutionary Biology*, **16**, 188.

FREEBERG, T. M., DUNBAR, R. I. and ORD, T. J. 2012. Social complexity as a proximate and ultimate factor in communicative complexity. *Philosophical Transactions of the Royal Society of London. Series B, Biological Sciences,* **367,** 1785–1801.

FREEBERG, T. M. and KRAMS, I. 2015. Does social complexity link vocal complexity and cooperation? *Journal of Ornithology*, **156**, 125–132.

FREITAG, J., LUDWIG, G., ANDREINI, I., RÖSSLER, P. and BREER, H. 1998. Olfactory receptors in aquatic and terrestrial vertebrates. *Journal of Comparative Physiology A*, **183**, 635–650.

GARRICK, L. D. and LANG, J. W. 1977. Social signals and behaviors of adult alligators and crocodiles. *American Zoologist*, **17**, 225–239.

GEORGI, J. A. and SIPLA, J. S. 2008. Comparative and functional anatomy of balance in aquatic reptiles and birds. 233–256. *In* THEWISSEN J. G. M. and NUMMELA S. (eds). *Sensory evolution on the threshold: Adaptations in secondarily aquatic vertebrates*. University of California Press, 358 pp.

GITTLEMAN, J. L. 1991. Carnivore olfactory bulb size: allometry, phylogeny and ecology. *Journal of Zoology*, **225**, 253–272.

GOWER, D. J. and SENNIKOV, A. G. 1996. Endocranial casts of early archosaurian reptiles. *Paläontologische Zeitschrift*, **70**, 579–589.

HAMMER, Ø., HARPER, D. A. T. and RYAN, P. D. 2001. PAST: Paleontological Statistics software package for education and data analysis. *Palaeontologia Electronica*, **4**, 9.

HARMON, L. J., WEIR, J. T., BROCK, C. D., GLOR, R. E. and CHALLENGER, W. 2007. GEIGER: investigating evolutionary radiations. *Bioinformatics*, **24**, 129-131.

HEMILA, S. and REUTER, T. 2008. The physics and biology of olfaction and taste. 29–34. *In* THEWISSEN J. G. M. and NUMMELA S. (eds). *Sensory evolution on the threshold: Adaptations in secondarily aquatic vertebrates*. University of California Press, 358 pp.

HOLLOWAY, W. L., CLAESON, K. M. and O'KEEFE, F. R. 2013. A virtual phytosaur endocast and its implications for sensory system evolution in archosaurs. *Journal of Vertebrate Paleontology*, **33**, 848–857.

HUA, S. and DE BUFFRENIL, V. 1996. Bone histology as a clue in the interpretation of functional adaptations in the Thalattosuchia (Reptilia, Crocodylia). *Journal of Vertebrate Paleontology*, **16**, 703–717.

HULLAR, T. E. 2006. Semicircular canal geometry, afferent sensitivity, and animal behavior. *The Anatomical Record Part A: Discoveries in Molecular, Cellular, and Evolutionary Biology: An Official Publication of the American Association of Anatomists,* **288**, 466-472.

JABLONSKI, D. 1995. Assessing extinction rates. 25–44. *In* MAY, R. M. and LAWTON, J. H. (eds). *Extinction rates*, Oxford University Press, Oxford, 248 pp.

JI, Q., LUO, Z. X., YUAN, C. X. and TABRUM, A. R., 2006. A swimming mammaliaform from the Middle Jurassic and ecomorphological diversification of early mammals. *Science*, **311**, 1123-1127.

JIRAK, D. and JANACEK, J. 2017. Volume of the crocodilian brain and endocast during ontogeny. *PLoS ONE*, **12**, e0178491.

KAWABE, S., SHIMOKAWA, T., MIKI, H., OKAMOTO, T. and MATSUDA, S. 2009. A simple and accurate method for estimating the brain volume of birds: possible application in paleoneurology. *Brain, Behavior and Evolution*, **74**, 295–301.

KAWABE, S., SHIMOKAWA, T., MIKI, H., MATSUDA, S. and ENDO, H. 2013. Variation in avian brain shape: relationship with size and orbital shape. *Journal of Anatomy*, **223**, 495-508.

KLEY, N. J., SERTICH, J. J., TURNER, A. H., KRAUSE, D. W., O'CONNOR, P. M. and GEORGI, J. A. 2010. Craniofacial morphology of *Simosuchus clarki* (Crocodyliformes: Notosuchia) from the Late Cretaceous of Madagascar. *Journal of Vertebrate Paleontology*, **30**, 13–98.

KRAUSE, E. T., KRUGER, O., KOHLMEIER, P. and CASPERS, B. A. 2012. Olfactory kin recognition in a songbird. *Biology Letters*, **8**, 327–329.

KUNDRÁT, M. 2007. Avian-like attributes of a virtual brain model of the oviraptorid theropod *Conchoraptor gracilis*. *Naturwissenschaften*, **94**, 499–504.

LAUDER, G. V. and NORTON, S. 1980. Asymmetrical muscle activity during feeding in the gar, *Lepisosteus oculatus*. *Journal of Experimental Biology*, **84**, 17–32.

LAUTENSCHLAGER, S., RAYFIELD, E. J., ALTANGEREL, P., ZANNO, L. E. and WITMER, L. M. 2012. The endocranial anatomy of Therizinosauria and its implications for sensory and cognitive function. *PLoS One*, **7**, e52289.

LAUTENSCHLAGER, S. 2014. Morphological and functional diversity in therizinosaur claws and the implications for theropod claw evolution. *Proceedings of the Royal Society of London B: Biological Sciences*, **281**, 20140497.

LAUTENSCHLAGER, S., BRIGHT, J. A. and RAYFIELD, E. J. 2014. Digital dissection–using contrast-enhanced computed tomography scanning to elucidate hard-and soft-tissue anatomy in the Common Buzzard *Buteo buteo*. *Journal of Anatomy*, **224**, 412-431.

LAUTENSCHLAGER, S. and BUTLER, R. J., 2016. Neural and endocranial anatomy of Triassic phytosaurian reptiles and convergence with fossil and modern crocodylians. *PeerJ*, **4**, e2251.

LAUTENSCHLAGER, S., FERREIRA, G. S. and WERNEBURG, I. 2018. Sensory evolution and ecology of early turtles revealed by digital endocranial reconstructions. *Frontiers in Ecology and Evolution,* **6**, 7.

LEAHEY, L. G., MOLNAR, R. E., CARPENTER, K., WITMER, L. M. and SALISBURY, S. W. 2015. Cranial osteology of the ankylosaurian dinosaur formerly known as *Minmi sp.* (Ornithischia: Thyreophora) from the Lower Cretaceous Allaru Mudstone of Richmond, Queensland, Australia. *PeerJ*, **3**, e1475.

LEARDI, J. M., POL, D. and CLARK, J. M. 2017. Detailed anatomy of the braincase of *Macelognathus vagans* Marsh, 1884 (Archosauria, Crocodylomorpha) using high resolution tomography and new insights on basal crocodylomorph phylogeny. *PeerJ*, **5**, e2801.

MALLON, J. C. 2017. Recognizing sexual dimorphism in the fossil record: lessons from nonavian dinosaurs. *Paleobiology*, **43**, 495–507.

MAREK, R. D., MOON, B. C., WILLIAMS, M. and BENTON, M. J. 2015. The skull and endocranium of a Lower Jurassic ichthyosaur based on digital reconstructions. *Palaeontology,* **58**, 723–742.

MARUGÁN-LOBÓN, J., CHIAPPE, L. M. and FARKE, A. A. 2013. The variability of inner ear orientation in saurischian dinosaurs: testing the use of semicircular canals as a reference system for comparative anatomy. *PeerJ*, **1**, e124.

MASON, N. A. and BURNS, K. J. 2015. The effect of habitat and body size on the evolution of vocal displays in Thraupidae (tanagers), the largest family of songbirds. *Biological Journal of the Linnean Society*, **114**, 538–551.

MILIÁN-GARCÍA, Y., VENEGAS-ANAYA, M., FRIAS-SOLER, R., CRAWFORD, A. V. J., RAMOS-TARGARONA, R., RODRÍGUEZ-SOBERÓN, R., ALONSO-TABET, M., THORBIARNARSON, J., SANIUR, O. I., ESPINOSA-LÓPEZ, G. and BERMINGHAM, E. 2011. Evolutionary history of Cuban crocodiles *Crocodylus rhombifer* and *Crocodylus acutus* inferred from multilocus markers. *Journal of Experimental Zoology Part A*, **315**, 358–375.

MÜLLER, J., BICKELMANN, C. and SOBRAL, G. 2018. The evolution and fossil history of sensory perception in amniote vertebrates. *Annual Review of Earth and Planetary Sciences*, **46**, 495–519.

NARINS, P. M., FENG, A. S., LIN, W., SCHNITZLER, H. U., DENZINGER, A., SUTHERS, R. A. and XU, C. 2004. Old World frog and bird vocalizations contain prominent ultrasonic harmonics. *The Journal of the Acoustical Society of America*, **115**, 910–913.

NEENAN, J. M. and SCHEYER, T. M. 2012. The braincase and inner ear of *Placodus gigas* (Sauropterygia, Placodontia)—a new reconstruction based on micro-computed tomographic data. *Journal of Vertebrate Paleontology*, **32**, 1350–1357.

NEENAN, J. M., REICH, T., EVERS, S. W., DRUCKENMILLER, P. S., VOETEN, D. F., CHOINIERE, J. N., BARRETT, P. M., PIERCE, S. E. and BENSON, R. B. 2017. Evolution of the sauropterygian labyrinth with increasingly pelagic lifestyles. *Current Biology*, **27**, 3852–3858.

NEENAN, J. M., CHAPELLE, K. E., FERNANDEZ, V. and CHOINIERE, J. N. 2019. Ontogeny of the *Massospondylus* labyrinth: implications for locomotory shifts in a basal sauropodomorph dinosaur. *Palaeontology*, **62**, 255-265.

NESBITT, S. J. 2011. The early evolution of archosaurs: relationships and the origin of major clades. *Bulletin of the American Museum of Natural History*, **352**, 1–292.

NESBITT, S. J., STOCKER, M. R., SMALL, B. J. and DOWNS, A. 2009. The osteology and relationships of *Vancleavea campi* (Reptilia: Archosauriformes). *Zoological Journal of the Linnean Society*, **157**, 814–864.

NICHOLLS, J. A. and GOLDIZEN, A. W. 2006. Habitat type and density influence vocal signal design in satin bowerbirds. *Journal of Animal Ecology*, **75**, 549–558.

O'BRIEN, H. D., FAITH, J. T., JENKINS, K. E., PEPPE, D. J., PLUMMER, T. W., JACOBS, Z. L., LI, B., JOANNES-BOYAU, R., PRICE, G., FENG, Y. X. and TRYON, C. A. 2016. Unexpected convergent evolution of nasal domes between Pleistocene bovids and Cretaceous hadrosaur dinosaurs. *Current Biology*, **26**, 503-508.

PARADIS, E., CLAUDE, J. and STRIMMER, K. 2004. APE: analyses of phylogenetics and evolution in R language. *Bioinformatics*, **20**, 289-290.

PIERCE, S. E., ANGIELCZYK, K. D. and RAYFIELD, E. J. 2008. Patterns of morphospace occupation and mechanical performance in extant crocodilian skulls: a combined geometric morphometric and finite element modeling approach. *Journal of morphology*, **269**, 840–864.

PIERCE, S. E., WILLIAMS, M. and BENSON, R. B. J. 2017. Virtual reconstruction of the endocranial anatomy of the early Jurassic marine crocodylomorph *Pelagosaurus typus* (Thalattosuchia). *PeerJ*, **5**, e3225.

PINHEIRO, F. L., FRANCA, M. A., LACERDA, M. B., BUTLER, R. J. and SCHULTZ, C. L. 2016. An exceptional fossil skull from South America and the origins of the archosauriform radiation. *Scientific Reports*, **6**, 22817.

PINHEIRO, J., BATES, D., DEBROY, S., SARKAR, D. and TEAM, R.C. 2018. NLME: linear and nonlinear mixed effects models. R package version 3.1-137.

PLATT, S. G., RAINWATER, T. R., FINGER, A. G., THORBIARNSARSON, J. B., ANDERSON, T. A. and MCMURRY, S. T. 2006. Food habits, ontogenetic dietary partitioning and observations of foraging behaviour of Morelet's crocodile (*Crocodylus moreletii*) in northern Belize. *The Herpetological Journal*, **16**, 281–290.

POLIHRONAKIS, M. 2006. Morphometric analysis of intraspecific shape variation in male and female genitalia of *Phyllophaga hirticula* (Coleoptera: Scarabaeidae: Melolonthinae). *Annals of the Entomological Society of America*, **99**, 144–150.

PRITZ, M. B. 1975. Anatomical identification of a telencephalic visual area in crocodiles: ascending connections of nucleus rotundus in *Caiman crocodilus*. *Journal of Comparative Neurology*, **164**, 323–338.

RAMAJO, L. BALTANÁS, Á., TORRES, R., MANRÍQUEZ, P. H., RODRIGUES-NAVARRO, A. and LAGOS, N. A. 2013. Geographical variation in shell morphology of juvenile snails (*Concholepas concholepas*) along the physical–chemical gradient of the Chilean coast. *Journal of the Marine Biological Association of the United Kingdom*, **93**, 2167–2176.

RAUP, D. M. 1979. Size of the Permo-Triassic bottleneck and its evolutionary implications. *Science*, **206**, 217-218.

RAY, S., CHINSAMY, A. and BANDYOPADHYAY, S. 2005. *Lystrosaurus murrayi* (Therapsida, Dicynodontia): bone histology, growth and lifestyle adaptations. *Palaeontology*, **48**, 1169-1185.

RAYFIELD, E. J. and MILNER, A. C. 2008. Establishing a framework for archosaur cranial mechanics. *Paleobiology*, **34**, 494–515.

REIG, O. A. 1970. The Proterosuchia and the early evolution of the archosaurs; an essay about the origin of a major taxon. *Bulletin of the Museum of Comparative Zoology*, **139**, 229–292.

RETALLACK, G. J., SMITH, R. M. H. and WARD, P. D. 2003. Vertebrate extinction across Permian–Triassic boundary in Karoo Basin, South Africa. *Geological Society of America Bulletin,* **115**, 1133-1152.

REVELL, L. J. 2012. phytools: an R package for phylogenetic comparative biology (and other things). *Methods in Ecology and Evolution*, **3**, 217-223.

ROGERS, S. W. 1998. Exploring dinosaur neuropaleobiology: computed tomography scanning and analysis of an *Allosaurus fragilis* endocast. *Neuron*, **21**, 673–679.

ROHLF, F. 2010. TPSDig2, Version 2.31. New York, NY, Stony Brook.

SALES, M. A. and SCHULTZ, C. L. 2014. Paleoneurology of *Teyumbaita sulcognathus* (Diapsida: Archosauromorpha) and the sense of smell in rhynchosaurs. *Palaeontologia Electronica*, **17**, 1–10.

SAMPSON, S. D. and WITMER, L. M. 2007. Craniofacial anatomy of *Majungasaurus crenatissimus* (Theropoda: Abelisauridae) from the late Cretaceous of Madagascar. *Journal of Vertebrate Paleontology*, **27**, 32–102.

SCHELLHORN, R. 2018. A potential link between lateral semicircular canal orientation, head posture, and dietary habits in extant rhinos (Perissodactyla, Rhinocerotidae). *Journal of Morphology*, **279**, 50-61.

SERENO, P. C. 1991. Basal archosaurs: phylogenetic relationships and functional implications. *Journal of Vertebrate Paleontology*, **11**, 1–53.

SERENO, P. C., WILSON, J. A., WITMER, L. M., WHITLOCK, J. A., MAGA, A., IDE, O. and ROWE, T. A. 2007. Structural extremes in a Cretaceous dinosaur. *PLoS ONE*, **2**, e1230.

SERRANO-MARTÍNEZ, A., KNOLL, F., NARVÁEZ, I., LAUTENSCHLAGER, S. and ORTEGA, F. 2019. Inner skull cavities of the basal eusuchian *Lohuecosuchus megadontos* (Upper Cretaceous, Spain) and neurosensorial implications. *Cretaceous Research*, **93**, 66-77.

SEWALL, K. B. 2015. Social complexity as a driver of communication and cognition. *Integrative and Comparative biology*, **55**, 384–395.

SMITH, R. M. H. 1995. Changing fluvial environments across the Permian-Triassic boundary in the Karoo Basin, South Africa and possible causes of tetrapod extinctions. *Palaeogeography, Palaeoclimatology, Palaeoecology*, **117**, 81–104.

SMITH, R. M. H. and BOTHA, J. 2005. The recovery of terrestrial vertebrate diversity in the South African Karoo Basin after the end-Permian extinction. *Comptes Rendus Palevol*, **4**, 623–636.

SMITH, R. M. H. and BOTHA-BRINK, J. 2014. Anatomy of a mass extinction: sedimentological and taphonomic evidence for drought-induced die-offs at the Permo-Triassic boundary in the main Karoo Basin, South Africa. *Palaeogeography, Palaeoclimatology, Palaeoecology*, **396**, 99-118.

SMITH, R. M. H. and WARD, P. D. 2001. Pattern of vertebrate extinctions across an event bed at the Permian-Triassic boundary in the Karoo Basin of South Africa. *Geology*, **29**, 1147–1150.

SMITH, R. M. H., RUBIDGE, B. and VAN DER WALT, M. 2012. Therapsid biodiversity patterns and palaeoenvironments of the Karoo Basin, South Africa. 31–64. *In* CHINSAMY-TURAN, A. (ed). *Forerunners of mammals: radiation, histology, biology*. Indiana University Press, Bloomington. 372 pp.

SOBRAL, G. and MÜLLER, J. 2017. Archosaurs and their kin: the ruling reptiles. 285–326. *In* CLACK, J. A., FAY, R. R., POPPER, A. N. (eds). *Evolution of the Vertebrate Ear*, Springer, 355 pp.

SOBRAL, G., SOOKIAS, R. B., BHULLAR, B. A. S., SMITH, R., BUTLER, R. J. and MÜLLER, J. 2016a. New information on the braincase and inner ear of *Euparkeria capensis* Broom: implications for diapsid and archosaur evolution. *Royal Society Open Science*, **3**, 160072.

SOBRAL, G., REISZ, R., NEENAN, J. M., MÜLLER, J. and SCHEYER, T. M. 2016b. Basal Reptilians, Marine Diapsids, and Turtles: The Flowering of Reptile Diversity. 207–243. *In* CLACK, J. A., FAY, R. R., POPPER, A. N. (eds). *Evolution of the vertebrate ear*. Springer, 355 pp.

STEIGER, S. S., KURYSHEV, V. Y., STENSMYR M. C., KEMPENAERS, B., MUELLER, J. C. 2009. A comparison of reptilian and avian olfactory receptor gene repertoires: species-specific expansion of group γ genes in birds. *BMC Genomics*, **10**, 446.

TATARINOV, L. P. 1961. Pseudosuchians of the USSR. *Paleontologicheskii Zhurnal*, **1961**, 117–132.

TAYLOR, M. P., WEDEL, M. J. and NAISH, D. 2009. Head and neck posture in sauropod dinosaurs inferred from extant animals. *Acta Palaeontologica Polonica*, **54**, 213–220.

THERRIEN, F., HENDERSON, D. M. and RUFF, C. B. 2005. Bite me: Biomechanical models of theropod mandibles and implications for feeding behaviour. 179–237. *In* CARPENTER, K. (ed). *The carnivorous dinosaurs*. Indiana University Press, Bloomington, 371 pp.

TROTTEYN, M. J. and PAULINA-CARABAJAL, A. 2016. Braincase and neuroanatomy of *Pseudochampsa ischigualastensis* and *Tropidosuchus romeri* (Archosauriformes, Proterochampsia). *Ameghiniana*, **53**, 527–542.

VERGNE, A. L., PRITZ, M. B. and MATHEYON, N. 2009. Acoustic communication in crocodilians: from behaviour to brain. *Biological Reviews*, **84**, 391-411.

VIDAL, D., ORTEGA, F. and SANZ, J. L. 2014. Titanosaur osteoderms from the Upper Cretaceous of Lo Hueco (Spain) and their implications on the armor of Laurasian titanosaurs. *PLoS ONE*, **9**, e102488.

VIGLIETTI, P. A., SMITH, R. M. and COMPTON, J. S. 2013. Origin and palaeoenvironmental significance of *Lystrosaurus* bonebeds in the earliest Triassic Karoo Basin, South Africa. *Palaeogeography, Palaeoclimatology, Palaeoecology*, **392**, 9–21.

VULLO, R., ALLAIN, R. and CAVIN, L. 2016. Convergent evolution of jaws between spinosaurid dinosaurs and pike conger eels. *Acta Palaeontologica Polonica*, **61**, 825-829.

WALSH, S. A., BARRETT, P. M., MILNER, A. C., MANLEY, G. and WITMER, L. M. 2009. Inner ear anatomy is a proxy for deducing auditory capability and behaviour in reptiles and birds. *Proceedings of the Royal Society of London B: Biological Sciences*, **276,** 1355–1360.

WALSH, S. A., LUO, Z. X. and BARRETT, P. M. 2013. Modern imaging techniques as a window to prehistoric auditory worlds. 227-261. *In* KOPPL, C., MANLEY, G., POPPER, A. N. and FAY, R. R. (eds). *Insights from Comparative Hearing Research.* Springer, 396 pp.

WELDON, P. J., SWENSON, D. J., OLSON, J. K. and BRINKMEIER, W. G. 1990. The American alligator detects food chemicals in aquatic and terrestrial environments. *Ethology*, **85**, 191–198.

WELMAN, J. 1998. The taxonomy of the South African proterosuchids (Reptilia, Archosauromorpha). *Journal of Vertebrate Paleontology*, **18**, 340–347.

WHARTON, D. S. 2000. An enlarged endocranial venous system in *Steneosaurus pictaviensis* (Crocodylia: Thalattosuchia) from the Upper Jurassic of Les Lourdines, France. *Comptes Rendus de l'Académie des Sciences-Series IIA-Earth and Planetary Science*, **331**, 221–226.

WITMER, L. M. and RIDGELY, R. C. 2009. New insights into the brain, braincase, and ear region of tyrannosaurs (Dinosauria, Theropoda), with implications for sensory organization and behavior. *The Anatomical Record*, **292**, 1266–1296.

WITMER, L. M., CHATTERJEE, S., FRANZOSA, J. and ROWE, T. 2003. Neuroanatomy of flying reptiles and implications for flight, posture and behaviour. *Nature*, **425**, 950–953.

WITMER, L. M., RIDGELY, R. C., DUFEAU, D. L. and SEMONES, M. C. 2008. Using CT to peer into the past: 3D visualization of the brain and ear regions of birds, crocodiles, and nonavian dinosaurs. 67–87. *In* ENDO, H. and FREY, R. (eds). *Anatomical imaging: towards a new morphology.* Springer, 110 pp.

YI, H. and NORELL, M. A. 2015. The burrowing origin of modern snakes. *Science Advances*, **1**, e1500743.

ZAHAVI, A. 1975. Mate selection—a selection for a handicap. *Journal of Theoretical Biology*, **53**, 205–214.

ZAHAVI, A. 1977. The cost of honesty: further remarks on the handicap principle. *Journal of Theoretical Biology*, **67**, 603–605.

ZELENITSKY, D. K., THERRIEN, F. and KOBAYASHI, Y. 2009. Olfactory acuity in theropods: palaeobiological and evolutionary implications. *Proceedings of the Royal Society of London B: Biological Sciences*, **276**, 667–673.

FIG 1. Specimens of *Proterosuchus fergusi* analysed in this study. A–D, SNSB-BSPG 1934 VIII 514; E–H, RC 846 (proposed neotype). Skulls are shown as photographs in dorsal (A, E),

right lateral (B, F), and left lateral (C, G) views, with outline drawings (D, H) of the most complete lateral view. Outline drawing of RC 846 (H) is taken from Ezcurra & Butler (2015a). All scale bars equal 50 mm.

FIG 2. Brain endocast reconstructions of *Proterosuchus fergusi*. (A–B) SNSB-BSPG 1934 VIII 514; (C–D) RC 846; (E–F) RC 846 μCT. Reconstructions show dorsal views of endocasts in situ (A, C, E), dorsal and left lateral views of isolated endocasts (B, D, F). Abbreviations: ca, carotid artery canal; cb, cerebellum; ch, cerebral hemispheres; el, endosseous labyrinth; mcv, middle cerebral vein; mo, medulla oblongata; ob, olfactory bulb; ot, olfactory tract; iv, trochlear nerve canal; v, trigeminal nerve canal; vi, abducens nerve; vii, facial nerve canal. Colour key: cranial endocast (blue); endosseous labyrinth (pink); cranial nerves (yellow); arterial canals (red); smaller venous canals (dark blue). Scale bars: 50 mm (A, C); 25 mm (E); 10 mm (B, D, F).

FIG 3. Endosseous labyrinths of *Proterosuchus fergusi* from highest to lowest CT resolution. A, B, left (A) and right (B) labyrinths of RC 846 (μCT). C, D, left (C) and right (D) labyrinths of SNSB-BSPG 1934 VIII 514. E, F, left (E) and right (F) labyrinths of RC 846. Labyrinths are shown in (from left to right) lateral, dorsal, medial, anterior and posterior views. Abbreviations: asc, anterior semi-circular canal; cc, crus communis; ecd, endosseous cochlear duct; fv, fenestra vestibuli; lsc, lateral semi-circular canal; psc, posterior semi-circular canal. All scale bars equal 5 mm.

FIG 4. Morphospace plots of archosauriform brain outlines based on elliptic Fourier analysis and after principal component analysis. Abbreviations: NAAR, non-archosaurian

archosauriform; NPPS, non-phytosaurian pseudosuchians; PHYT, Phytosauria; PTER, Pterosauria; SAUR, Sauropodomorpha; ORTH, Ornithischia; NATH, non-avian theropods; AVES, Aves. † denotes extinct taxa. For taxonomic information see Brown *et al*. (2019, Fig. S9). Silhouettes used include work by S. Hartman, M. Witton, N. Tamura and T. M. Keesey (see http://phylopic.org for full licensing information).

FIG 5. Morphospace plots of avian and reptile inner ear outlines based on elliptic Fourier analysis and after principal component analysis, both with and without the endosseous cochlear duct (ECD). (A) with ECD; (B) without ECD. Colour key: Aquatic (dark blue); Semi-aquatic (light blue); Terrestrial (yellow). Abbreviations: SQUA, Squamata; SAUO, Sauropterygia; TEST, Testudines; NAAR, non-archosaurian archosauriform; PHYT, Phytosauria; NPPS, non-phytosaurian pseudosuchians; ORNI, Ornithischia; SAUR, Sauropodomorpha; NATH, non-avian theropods; AVES, Aves. For taxonomic information see Brown *et al*. (2019, Fig. S6).

FIG 6. Morphospace plots of avian and reptile semi-circular canal landmarks after principal component analysis. PC1 versus PC2. (A) ASC; (B) LSC; (C) PSC. For taxonomic information see Brown *et al*. (2019, fig. S9).

FIG 7. Discerning the 'alert' head posture in life from the orientation of the lateral semi-circular canal (LSC). (A) Orientation of the LSC when head posture of *Proterosuchus fergusi* is horizontal in both specimens studied. (B) Head posture of *P. fergusi* in life following mean average orientation of all LSC planes studied. (C) Comparative head posture of *Crocodylus johnstoni* following the orientation of the LSC plane (Witmer *et al.* 2008). *Proterosuchus*

fergusi and *C. johnstoni* skull figures modified from Ezcurra & Butler (2015a) and Witmer *et al.* (2008) respectively.

FIG 8. Correlation plot between scaled/log transformed ECD length and variables of hearing sensitivity for extant reptiles and Aves. Both a linear regression (solid line) and PGLS regression (dashed line) were used to estimate the auditory capabilities of *Proterosuchus fergusi* (indicated by the hollow circle). Sensitivity variables: (A) mean hearing frequency; (B) hearing range. Abbreviations: SQUA, Squamata; RHYN, Rhynchocephalia; TEST, Testudines; CROC, Crocodylomorpha; AVES, Aves. For taxonomic information see Brown *et al.* (2019, fig. S10).

FIG 9. Change in the resistance to dorsoventral bending (lx), mediolateral bending (ly), and torsion (J) along the rostra in *Proterosuchus fergusi* and comparative extant taxa. (A) log lx true size; (B) log lx scaled size; (C) log ly true size; (D) log ly scaled size; (E) log J true size; (F) log J scaled size. In *Proterosuchus fergusi*, both a straight beam (solid line) and a curved beam (dashed line) were used when analysing the anterior 20% of the rostrum.

FIG 10. Evolution of the brain cavity in Archosauriformes. Left lateral view of the brain cavity of saurians redrawn from the literature. (A) snake *Dispholidus typus* (Allemand *et al.* 2017); (B) *Proterosuchus fergusi* (this study); (C) proterochampsian *Tropidosuchus romeri* (Trotteyn & Paulina-Carabajal 2016); (D) *Parasuchus angustifrons* (retrodeformed, Lautenschlager & Butler 2016); (E) *Ebrachosuchus neukami* (retrodeformed, Lautenschlager & Butler 2016); (F) *Riojasuchus tenuisceps* (Baczko & Desojo 2016); (G) *Pelagosaurus typus* (Pierce *et al.* 2017); (H) *Caiman crocodilus* (Jirak & Janacek 2017); (I) *Crocodylus seamensis*

(Kawabe *et al.* 2009); (J) *Anhanguera santanae* (Witmer *et al.* 2003); (K) *Tyrannosaurus rex* (Witmer *et al.* 2008); (L) *Bubo virginianus* (Witmer *et al.* 2008). † denotes extinct taxa. Phylogeny following Nesbitt (2011) and Ezcurra (2016). Brain cavities not to scale.

FIG 11. Evolution of the endosseous labyrinth in Archosauriformes. Lateral view of the left labyrinth of archosauriforms redrawn from the literature. (A) snake *Ptyas mucosa* (reversed, Yi & Norell 2015); (B) *Proterosuchus fergusi* (this study); (C) proterochampsian *Tropidosuchus romeri* (reversed, Trotteyn & Paulina-Carabajal 2016); (D) *Euparkeria capensis* (reversed, Sobral *et al.* 2016); (E) *Parasuchus angustifrons* (retrodeformed, Lautenschlager & Butler 2016); (F) *Ebrachosuchus neukami* (retrodeformed, Lautenschlager & Butler 2016); (G) *Simosuchus clarki* (reversed, Kley 2010); (H) *Pelagosaurus typus* (Pierce *et al.* 2017); (I) *Steneosaurus cf. gracilirostris* (Brusatte *et al.* 2016); (J) *Crocodylus johnstoni* (Brusatte *et al.* 2016); (K) *Alligator mississippiensis* (Brusatte *et al.* 2016); (L) *Stegosaurus stenops* (Leahey *et al.* 2015); (M) *Camarasaurus lentus* (Witmer *et al.* 2008); (N) *Tyrannosaurus rex* (Witmer *et al.* 2008); (O) *Bubo virginianus* (Witmer *et al.* 2008). † denotes extinct taxa. Abbreviations: ASC, anterior semi-circular canal; ECD, endosseous cochlea duct; LSC, lateral semi-circular canal; PSC, posterior semi-circular canal. Phylogeny following Nesbitt (2011), Ezcurra (2016) and Leardi *et al.* (2017). Labyrinths not to scale.

Table 1. Results of one-way PERMANOVA test on endocranial outlines between ecological groupings using all axes. *Proterosuchus* is excluded. Results in bold show statistical significance at p = 0.05.

Permutation N	10000
Total sum of squares	6.193
Within-group sum of squares	5.098
F	7.082
p	0.0002

Ecological groupings	p-value (w/ ECD)
Aquatic/Semi-aquatic	0.0998
Aquatic/Terrestrial	0.4222
Semi-aquatic/Terrestrial	**<0.0001**

Table 2. Results of one-way PERMANOVA test on endocranial outlines between phylogenetic groupings and using all axes. Abbreviations: NAAR, non-archosaurian archosauriform; PHYT, Phytosauria; NPPS, non-phytosaurian pseudosuchians; PTER, Pterosauria; ORTH, Ornithischia; SAUR, Sauropodomorpha; NATH, non-avian theropods; AVES, Aves. Results in bold show statistical significance at p = 0.05.

Permutation N 10000

Total sum of squares 6.255

Within-group sum of squares 2.825

F 10.75

p 1.00E-04

p-values	PHYT	NPPS	PTER	ORNI	SAUR	NATH	AVES
NAAR	0.4312	0.7721	0.104	**0.0215**	**0.0190**	0.0612	**0.0064**
PHYT		0.1084	**0.0183**	**0.0043**	**0.0033**	**0.0175**	**0.0002**
NPPS			**0.0015**	**0.0001**	**0.0001**	**0.0002**	**0.0001**
PTER				**0.0126**	**0.0310**	**0.0136**	**0.0406**
ORNI					**0.0086**	**0.0263**	**0.0001**
SAUR						**0.0014**	**0.0001**
NATH							**0.0001**

Table 3. Results of one-way PERMANOVA test on inner ear outlines between ecological groupings with (left) and without (right) the endosseous cochlea duct (ECD) and using all axes. *Proterosuchus* is excluded. Results in bold show statistical significance at p = 0.05.

Permutation N 10000/10000

Total sum of squares 7.52/ 5.685

Within-group sum of squares 6.546/ 5.315

F 6.772/ 3.345

p 0.0001/ 0.0044

Ecological groupings	p-value (w/ ECD)	p-value (w/o ECD)
Aquatic/Semi-aquatic	**0.0099**	**0.0282**
Aquatic/Terrestrial	**0.0003**	**0.0013**
Semi-aquatic/Terrestrial	**0.0099**	0.2968

Table 4. Results of one-way PERMANOVA test on inner ear outlines between phylogenetic groupings with (left) and without (right) the endosseous cochlea duct (ECD) and using all

axes. Abbreviations: SQUA, Squamata; SAUO, Sauropterygia; TEST, Testudines; NAAR, non-archosaurian archosauriform; PHYT, Phytosauria; NPPS, non-phytosaurian pseudosuchians; ORNI, Ornithischia; SAUR, Sauropodomorpha; NATH, non-avian theropods; AVES, Aves. Results in bold show statistical significance at p = 0.05.

Permutation N 10000

Total sum of squares 1.658

Within-group sum of squares 0.522

F 10.26

p 9.999E-05

p-values (w/o ECD \ w/ ECD)	SQUA	SAUO	TEST	NAAR	PHYT	NPPS	ORNI	SAUR	NATH	AVES
SQUA		**0.0002**	**0.0005**	**0.0010**	**0.0065**	**0.0001**	**0.0005**	**0.0001**	**0.0001**	**0.0001**
SAUO	**0.0101**		0.4432	0.2562	0.1680	**0.0002**	**0.0015**	**0.0001**	**0.0001**	**0.0001**
TEST	**0.0032**	**0.0307**		0.1189	0.1078	**0.0001**	**0.0014**	**0.0001**	**0.0001**	**0.0001**
NAAR	**0.0303**	0.3823	**0.0007**		0.0995	**0.0027**	**0.0290**	**0.0034**	**0.0014**	**0.0007**
PHYT	0.2860	0.6812	**0.0320**	0.7363		0.0671	0.1380	**0.0150**	**0.0119**	**0.0040**
NPPS	**0.0392**	0.3248	**0.0185**	0.1340	0.6042		**0.0023**	**0.0001**	**0.0001**	**0.0001**
ORNI	**0.0028**	0.3494	**0.0002**	**0.0063**	**0.0392**	**0.0072**		0.2123	**0.0080**	**0.0013**
SAUR	**0.0003**	**0.0200**	**0.0001**	0.0618	0.1232	**0.0001**	**0.0005**		0.1188	**0.0015**
NATH	**0.0001**	**0.0003**	**0.0001**	**0.0047**	**0.0162**	**0.0001**	**0.0001**	**0.0319**		**0.0011**
AVES	**0.0001**	**0.0001**	**0.0001**	**0.0004**	**0.0053**	**0.0001**	**0.0001**	**0.0001**	**0.0001**	

Table 5. Results of canonical variate analysis on semi-circular canal landmarks using all axes. *Proterosuchus* was excluded. Results in bold show statistical significance at p = 0.05.

Permutation N 10000

Ecological groupings	**ASC**		**LSC**		**PSC**	
	Procrustes	**p-value**	**Procrustes**	**p-value**	**Procrustes**	**p-value**
Terrestrial/Semi-Aquatic	0.1937	**0.0146**	0.1093	0.2442	0.1921	**0.0178**
Terrestrial/Aquatic	0.2970	**0.0002**	0.2646	**0.0050**	0.2168	**0.0051**
Semi-Aquatic/Aquatic	0.1655	**0.0075**	0.1778	**0.0314**	0.1099	0.3103

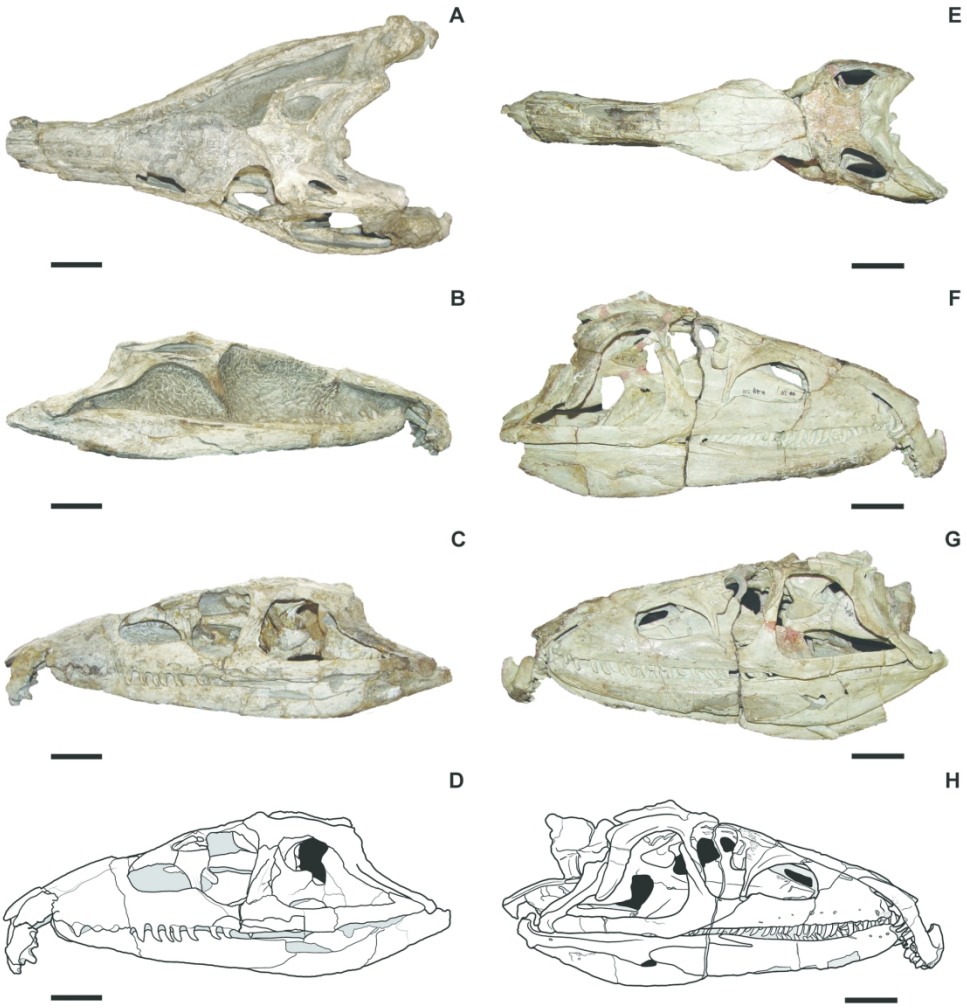

FIG 1. Specimens of Proterosuchus fergusi analysed in this study. A–D, SNSB-BSPG 1934 VIII 514; E–H, RC 846 (proposed neotype). Skulls are shown as photographs in dorsal (A, E), right lateral (B, F), and left lateral (C, G) views, with outline drawings (D, H) of the most complete lateral view. Outline drawing of RC 846 (H) is taken from Ezcurra & Butler (2015a). All scale bars equal 50 mm.

165x170mm (300 x 300 DPI)

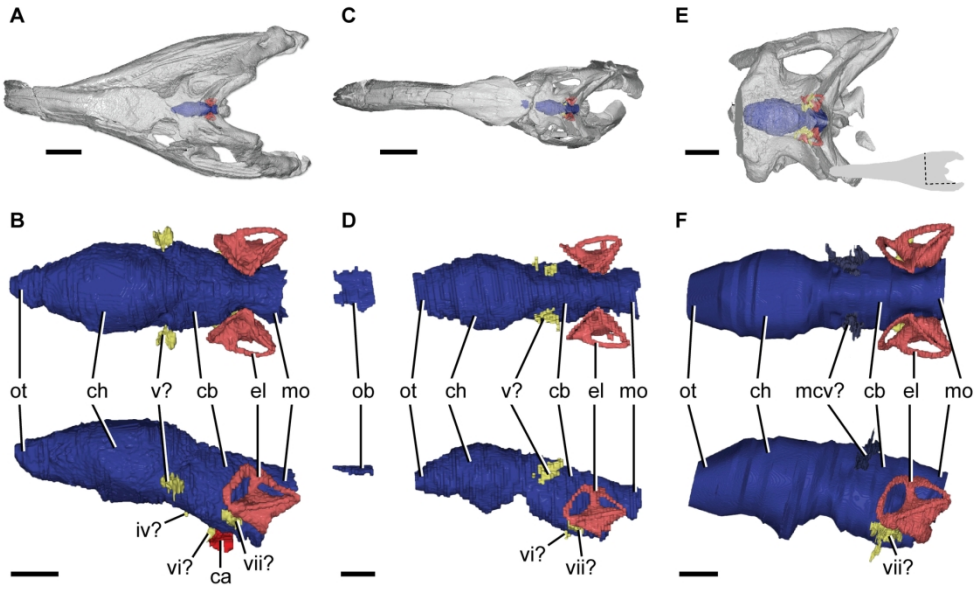

FIG 2. Brain endocast reconstructions of Proterosuchus fergusi. (A–B) SNSB-BSPG 1934 VIII 514; (C–D) RC 846; (E–F) RC 846 µCT. Reconstructions show dorsal views of endocasts in situ (A, C, E), dorsal and left lateral views of isolated endocasts (B, D, F). Abbreviations: ca, carotid artery canal; cb, cerebellum; ch, cerebral hemispheres; el, endosseous labyrinth; mcv, middle cerebral vein; mo, medulla oblongata; ob, olfactory bulb; ot, olfactory tract; iv, trochlear nerve canal; v, trigeminal nerve canal; vi, abducens nerve; vii, facial nerve canal. Colour key: cranial endocast (blue); endosseous labyrinth (pink); cranial nerves (yellow); arterial canals (red); smaller venous canals (dark blue). Scale bars: 50 mm (A, C); 25 mm (E); 10 mm (B, D, F).

170x100mm (300 x 300 DPI)

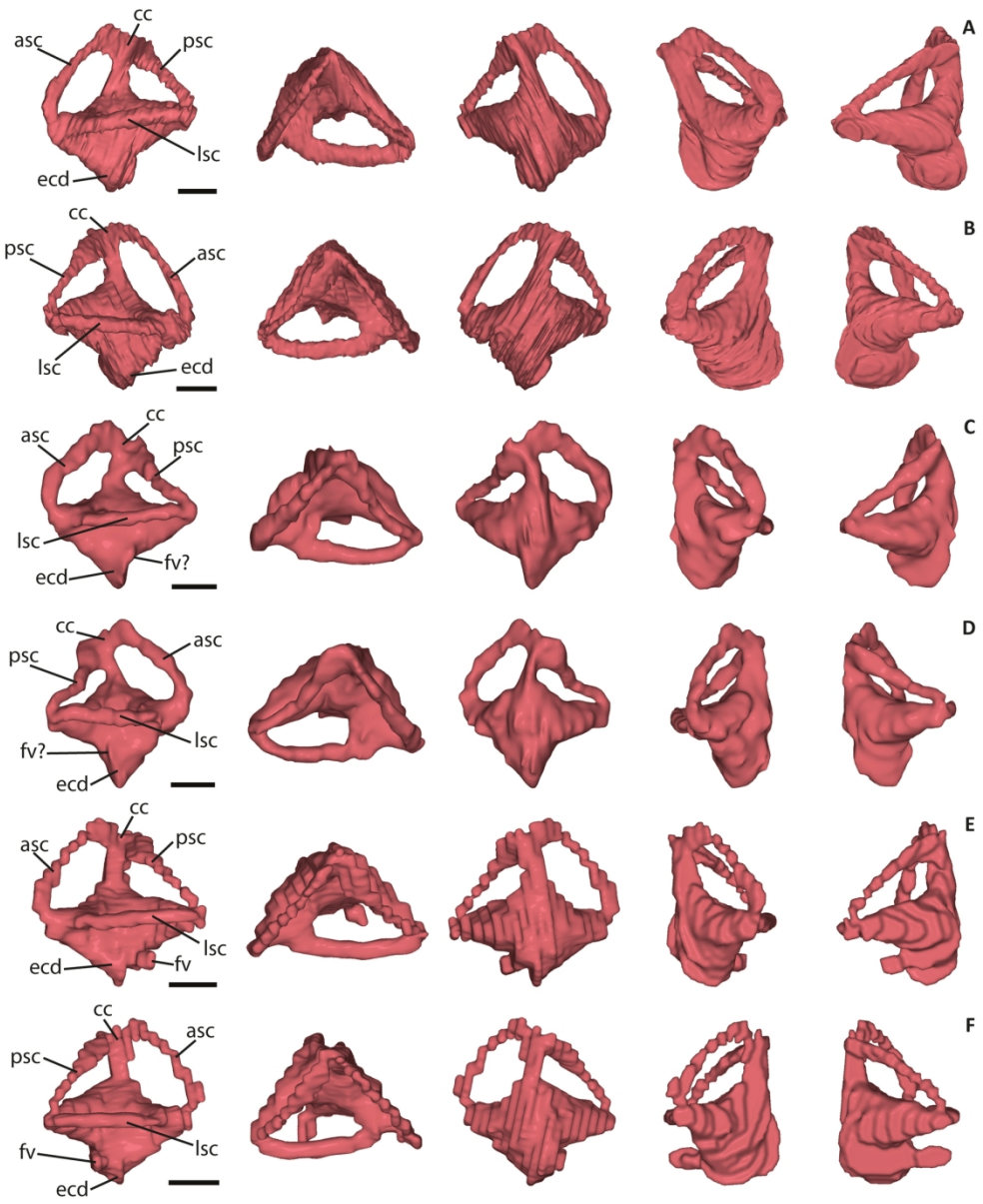

FIG 3. Endosseous labyrinths of Proterosuchus fergusi from highest to lowest CT resolution. A, B, left (A) and right (B) labyrinths of RC 846 (μCT). C, D, left (C) and right (D) labyrinths of SNSB-BSPG 1934 VIII 514. E, F, left (E) and right (F) labyrinths of RC 846. Labyrinths are shown in (from left to right) lateral, dorsal, medial, anterior and posterior views. Abbreviations: asc, anterior semi-circular canal; cc, crus communis; ecd, endosseous cochlear duct; fv, fenestra vestibuli; lsc, lateral semi-circular canal; psc, posterior semi-circular canal. All scale bars equal 5 mm.

161x194mm (300 x 300 DPI)

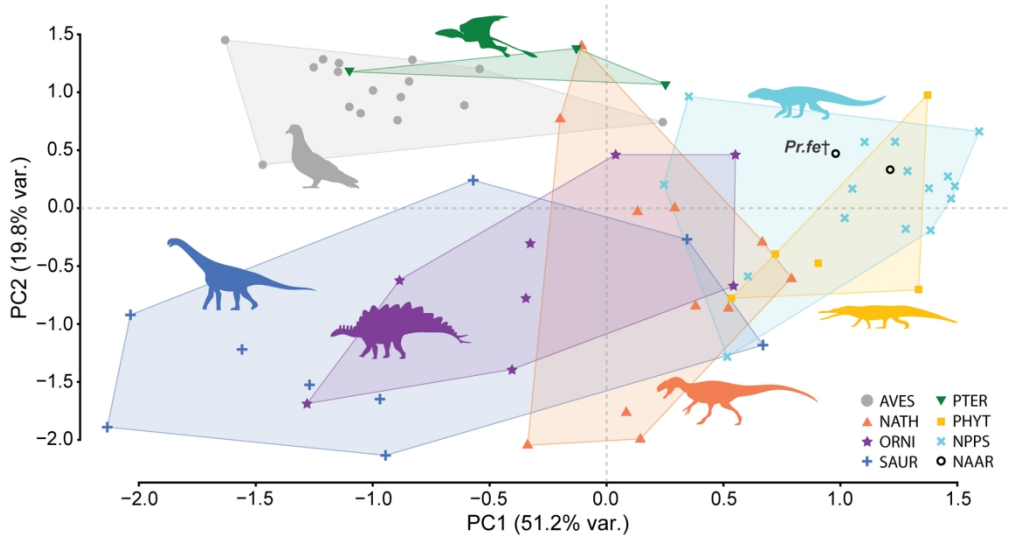

FIG 4. Morphospace plots of archosauriform brain outlines based on elliptic Fourier analysis and after principal component analysis. Abbreviations: NAAR, non-archosaurian archosauriform; NPPS, non-phytosaurian pseudosuchians; PHYT, Phytosauria; PTER, Pterosauria; SAUR, Sauropodomorpha; ORTH, Ornithischia; NATH, non-avian theropods; AVES, Aves. † denotes extinct taxa. For taxonomic information see Brown et al. (2019, Fig. S9). Silhouettes used include work by S. Hartman, M. Witton, N. Tamura and T. M. Keesey (see http://phylopic.org for full licensing information).

166x88mm (300 x 300 DPI)

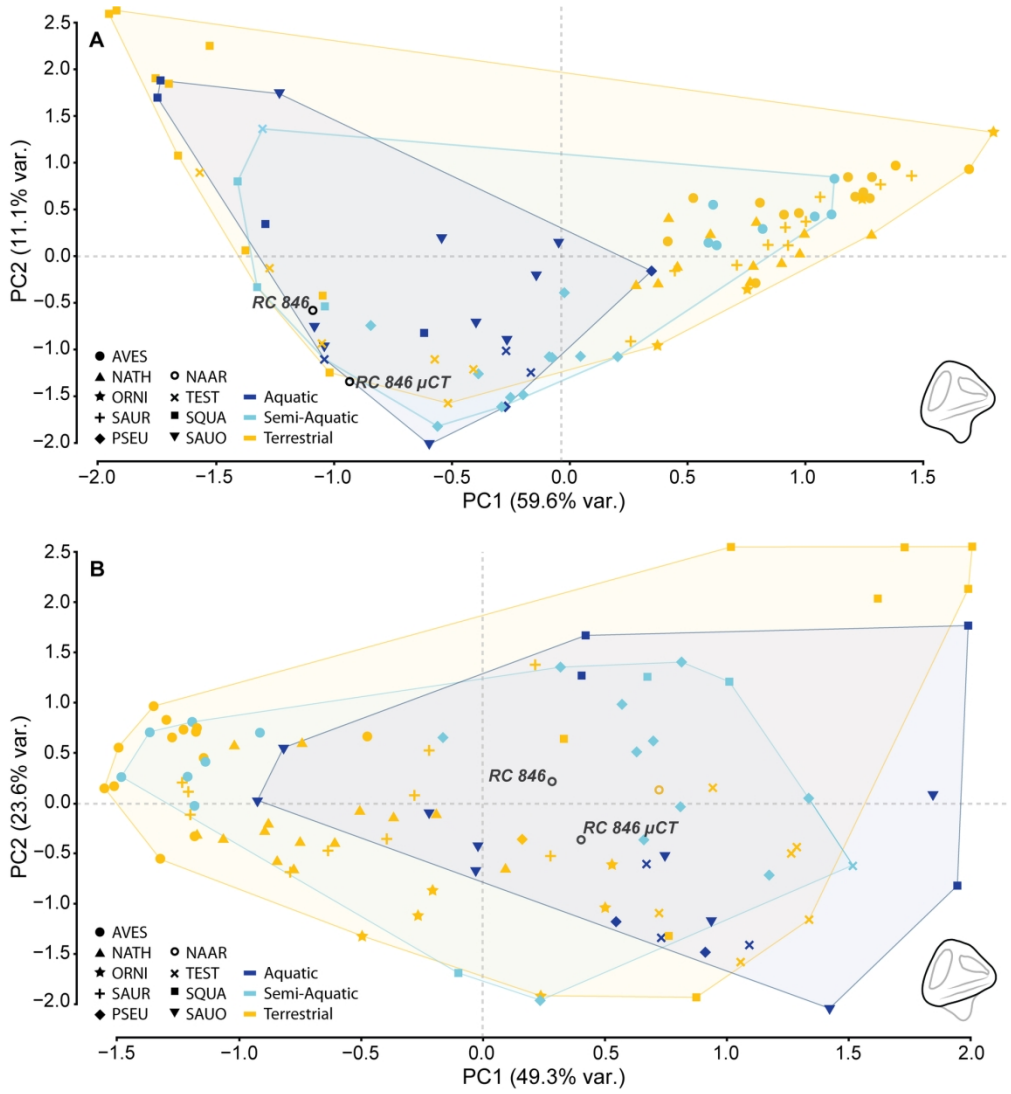

FIG 5. Morphospace plots of avian and reptile inner ear outlines based on elliptic Fourier analysis and after principal component analysis, both with and without the endosseous cochlear duct (ECD). (A) with ECD; (B) without ECD. Colour key: Aquatic (dark blue); Semi-aquatic (light blue); Terrestrial (yellow). Abbreviations: SQUA, Squamata; SAUO, Sauropterygia; TEST, Testudines; NAAR, non-archosaurian archosauriform; PHYT, Phytosauria; NPPS, non-phytosaurian pseudosuchians; ORNI, Ornithischia; SAUR, Sauropodomorpha; NATH, non-avian theropods; AVES, Aves. For taxonomic information see Brown et al. (2019, Fig. S6).

166x180mm (300 x 300 DPI)

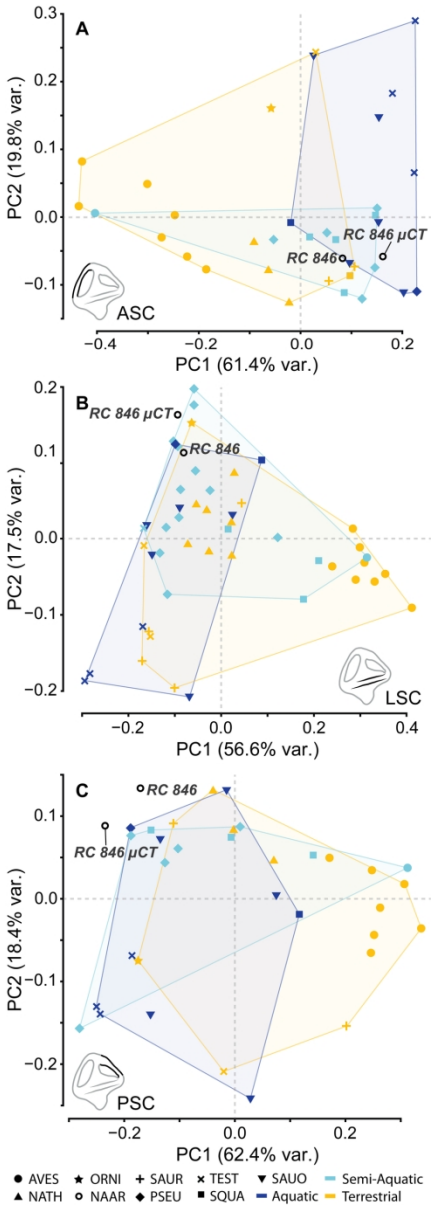

FIG 6. Morphospace plots of avian and reptile semi-circular canal landmarks after principal component analysis. PC1 versus PC2. (A) ASC; (B) LSC; (C) PSC. For taxonomic information see Brown et al. (2019, fig. S9).

80x226mm (300 x 300 DPI)

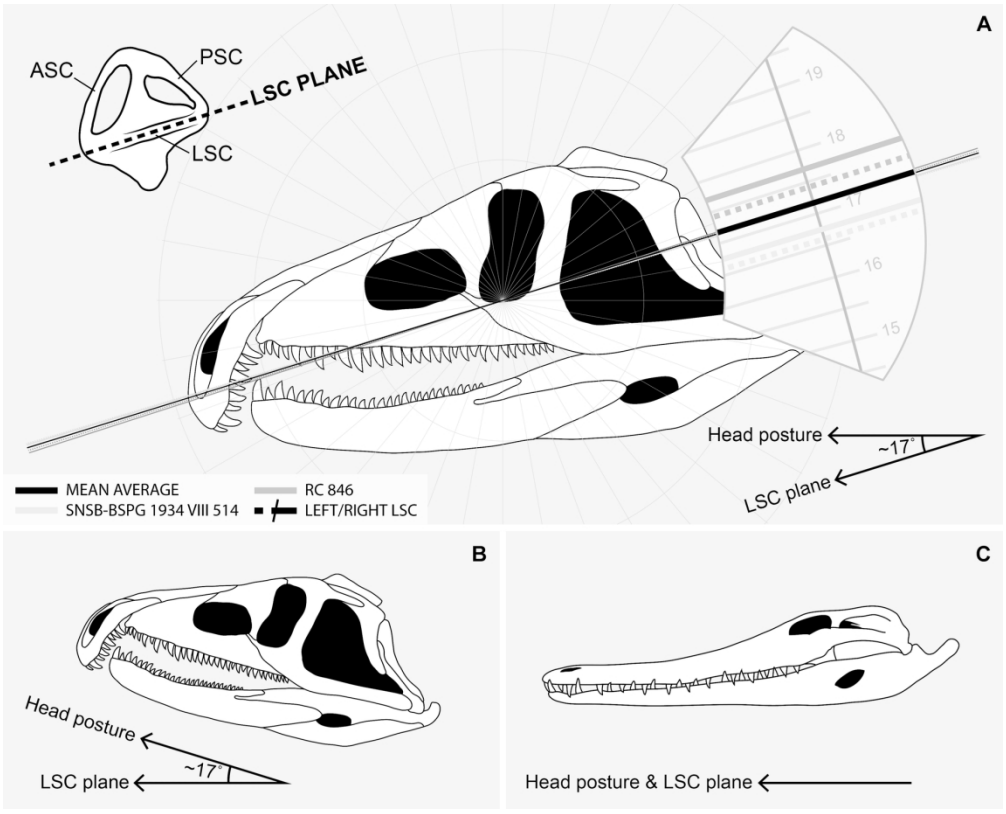

FIG 7. Discerning the 'alert' head posture in life from the orientation of the lateral semi-circular canal (LSC). (A) Orientation of the LSC when head posture of Proterosuchus fergusi is horizontal in both specimens studied. (B) Head posture of P. fergusi in life following mean average orientation of all LSC planes studied. (C) Comparative head posture of Crocodylus johnstoni following the orientation of the LSC plane (Witmer et al. 2008). Proterosuchus fergusi and C. johnstoni skull figures modified from Ezcurra & Butler (2015a) and Witmer et al. (2008) respectively.

165x133mm (300 x 300 DPI)

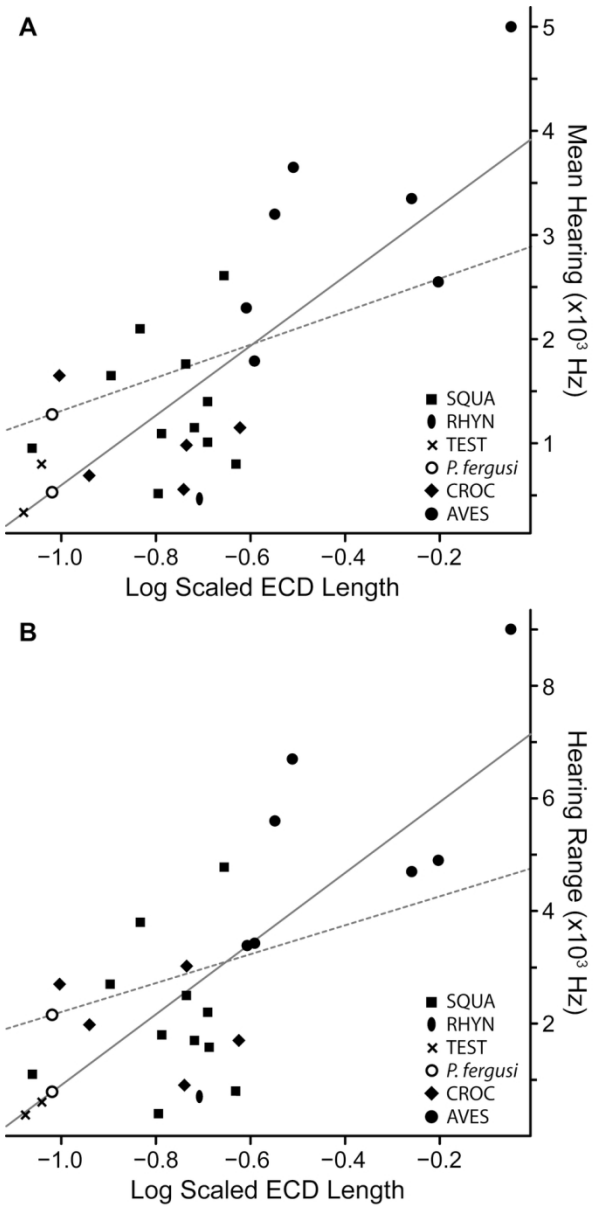

FIG 8. Correlation plot between scaled/log transformed ECD length and variables of hearing sensitivity for extant reptiles and Aves. Both a linear regression (solid line) and PGLS regression (dashed line) were used to estimate the auditory capabilities of Proterosuchus fergusi (indicated by the hollow circle). Sensitivity variables: (A) mean hearing frequency; (B) hearing range. Abbreviations: SQUA, Squamata; RHYN, Rhynchocephalia; TEST, Testudines; CROC, Crocodylomorpha; AVES, Aves. For taxonomic information see Brown et al. (2019, fig. S10).

81x165mm (300 x 300 DPI)

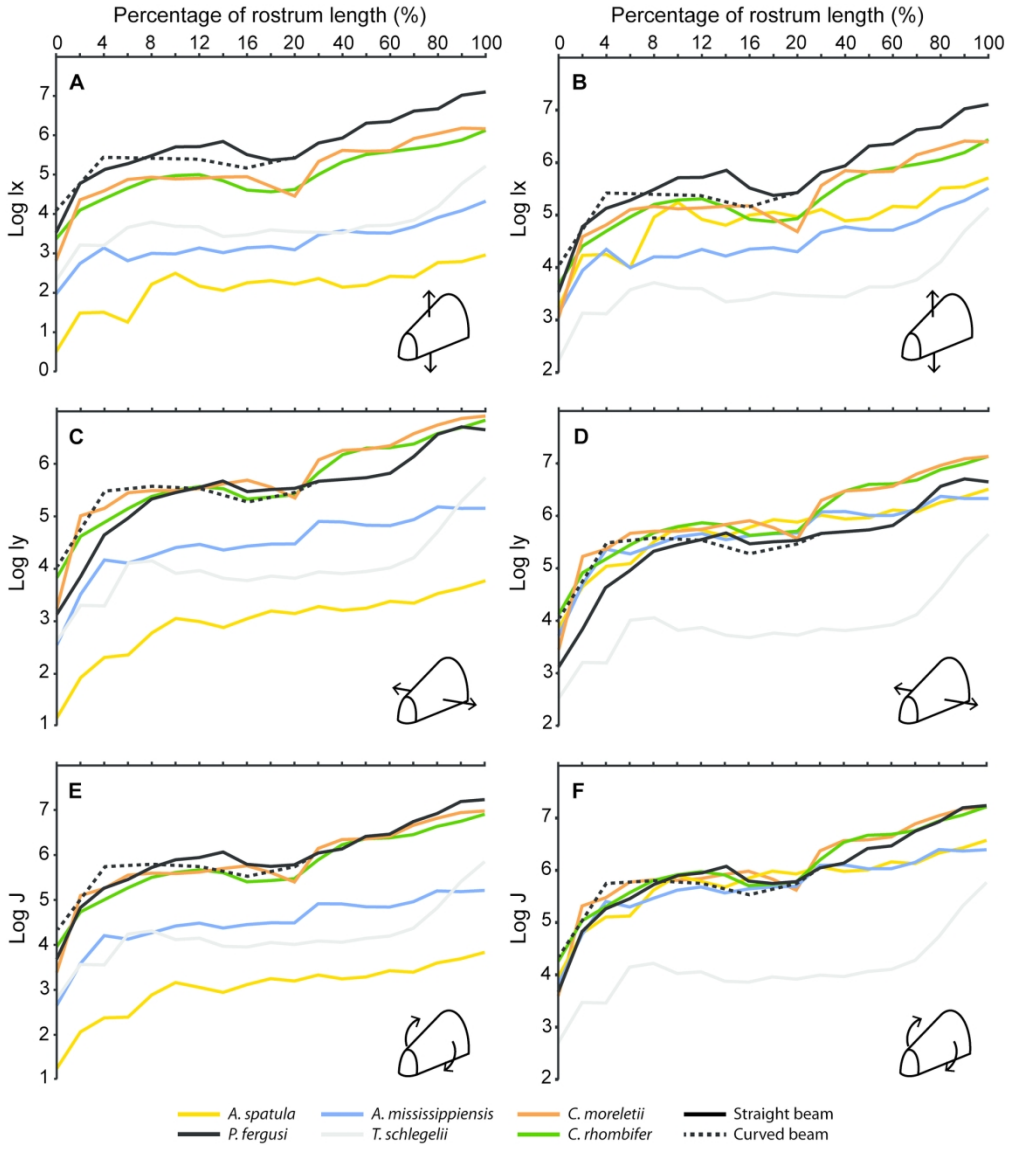

FIG 9. Change in the resistance to dorsoventral bending (lx), mediolateral bending (ly), and torsion (J) along the rostra in Proterosuchus fergusi and comparative extant taxa. (A) log lx true size; (B) log lx scaled size; (C) log ly true size; (D) log ly scaled size; (E) log J true size; (F) log J scaled size. In Proterosuchus fergusi, both a straight beam (solid line) and a curved beam (dashed line) were used when analysing the anterior 20% of the rostrum.

166x189mm (300 x 300 DPI)

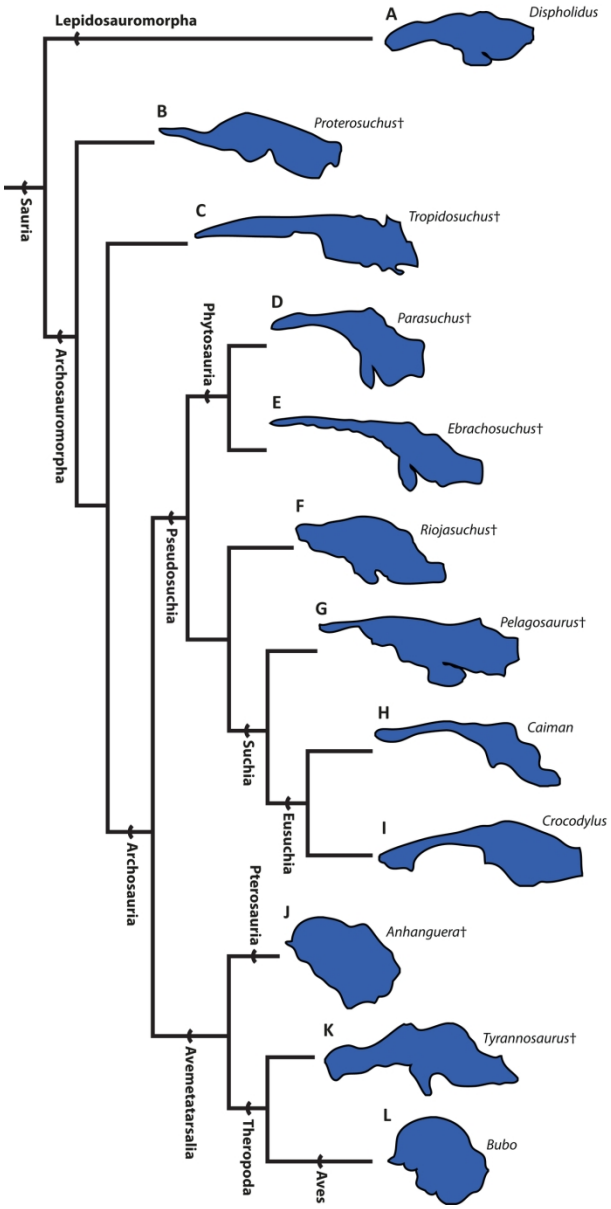

FIG 10. Evolution of the brain cavity in Archosauriformes. Left lateral view of the brain cavity of saurians redrawn from the literature. (A) snake Dispholidus typus (Allemand et al. 2017); (B) Proterosuchus fergusi (this study); (C) proterochampsian Tropidosuchus romeri (Trotteyn & Paulina-Carabajal 2016); (D) Parasuchus angustifrons (retrodeformed, Lautenschlager & Butler 2016); (E) Ebrachosuchus neukami (retrodeformed, Lautenschlager & Butler 2016); (F) Riojasuchus tenuisceps (Baczko & Desojo 2016); (G) Pelagosaurus typus (Pierce et al. 2017); (H) Caiman crocodilus (Jirak & Janacek 2017); (I) Crocodylus seamensis (Kawabe et al. 2009); (J) Anhanguera santanae (Witmer et al. 2003); (K) Tyrannosaurus rex (Witmer et al. 2008); (L) Bubo virginianus (Witmer et al. 2008). † denotes extinct taxa. Phylogeny following Nesbitt (2011) and Ezcurra (2016). Brain cavities not to scale.

109x217mm (300 x 300 DPI)

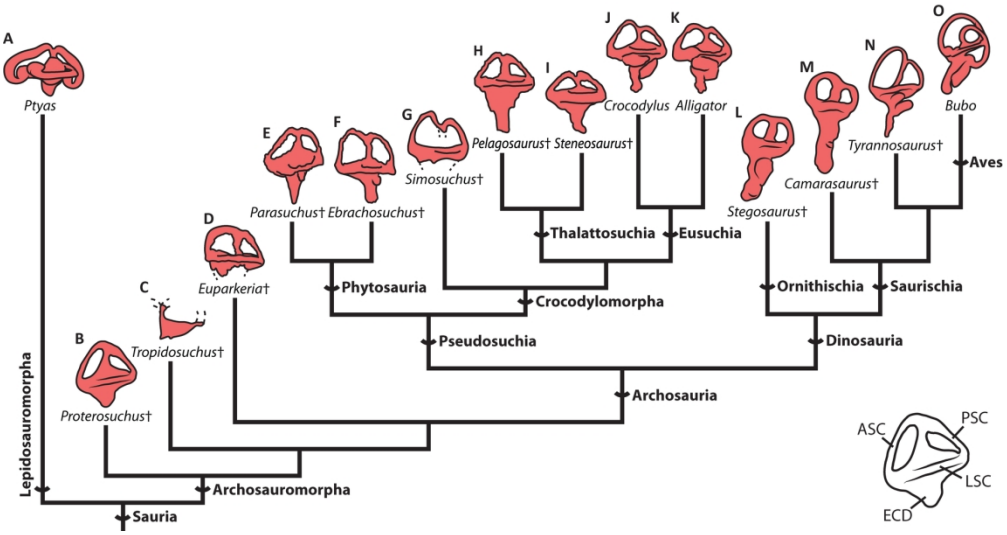

FIG 11. Evolution of the endosseous labyrinth in Archosauriformes. Lateral view of the left labyrinth of archosauriforms redrawn from the literature. (A) snake Ptyas mucosa (reversed, Yi & Norell 2015); (B) Proterosuchus fergusi (this study); (C) proterochampsian Tropidosuchus romeri (reversed, Trotteyn & Paulina-Carabajal 2016); (D) Euparkeria capensis (reversed, Sobral et al. 2016); (E) Parasuchus angustifrons (retrodeformed, Lautenschlager & Butler 2016); (F) Ebrachosuchus neukami (retrodeformed, Lautenschlager & Butler 2016); (G) Simosuchus clarki (reversed, Kley 2010); (H) Pelagosaurus typus (Pierce et al. 2017); (I) Steneosaurus cf. gracilirostris (Brusatte et al. 2016); (J) Crocodylus johnstoni (Brusatte et al. 2016); (K) Alligator mississippiensis (Brusatte et al. 2016); (L) Stegosaurus stenops (Leahey et al. 2015); (M) Camarasaurus lentus (Witmer et al. 2008); (N) Tyrannosaurus rex (Witmer et al. 2008); (O) Bubo virginianus (Witmer et al. 2008). † denotes extinct taxa. Abbreviations: ASC, anterior semi-circular canal; ECD, endosseous cochlea duct; LSC, lateral semi-circular canal; PSC, posterior semi-circular canal. Phylogeny following Nesbitt (2011), Ezcurra (2016) and Leardi et al. (2017). Labyrinths not to scale.

166x87mm (300 x 300 DPI)